The lipid phosphatase LPP3 regulates extra-embryonic vasculogenesis and axis patterning

Diana Escalante-Alcalde[1,*], Lidia Hernandez[1], Hervé Le Stunff[3], Ryu Maeda[2], Hyun-Shik Lee[2], Jr-Gang-Cheng[1], Vicki A. Sciorra[4], Ira Daar[2], Sarah Spiegel[3], Andrew J. Morris[4] and Colin L. Stewart[1,†]

[1]Cancer and Developmental Biology Laboratory and [2]Regulation of Cell Growth Laboratory, Division of Basic Science, National Cancer Institute, Frederick, MD 21702, USA
[3]Department of Biochemistry and Molecular Biophysics, Medical College of Virginia Campus, Virginia Commonwealth University, Richmond, VA 23298,USA
[4]Department of Cell and Developmental Biology, University of North Carolina at Chapel Hill, Chapel Hill, NC 27599-7090, USA
*Present address: Instituto de Fisiología Celular, UNAM, Ciudad Universitaria, 04510 México
†Author for correspondence (e-mail: stewartc@ncifcrdc.gov)

Accepted 29 May 2003

Development 130, 4623-4637
© 2003 The Company of Biologists Ltd
doi:10.1242/dev.00635

Summary

Bioactive phospholipids, which include sphingosine-1-phosphate, lysophosphatidic acid, ceramide and their derivatives regulate a wide variety of cellular functions in culture such as proliferation, apoptosis and differentiation. The availability of these lipids and their products is regulated by the lipid phosphate phosphatases (LPPs). Here we show that mouse embryos deficient for *LPP3* fail to form a chorio-allantoic placenta and yolk sac vasculature. A subset of embryos also show a shortening of the anterior-posterior axis and frequent duplication of axial structures that are strikingly similar to the phenotypes associated with *axin* deficiency, a critical regulator of Wnt signaling. Loss of *LPP3* results in a marked increase in β-catenin-mediated TCF transcription, whereas elevated levels of LPP3 inhibit β-catenin-mediated TCF transcription. LPP3 also inhibits axis duplication and leads to mild ventralization in *Xenopus* embryo development. Although *LPP3* null fibroblasts show altered levels of bioactive phospholipids, consistent with loss of LPP3 phosphatase activity, mutant forms of *LPP3*, specifically lacking phosphatase activity, were able to inhibit β-catenin-mediated TCF transcription and also suppress axis duplication, although not as effectively as intact LPP3. These results reveal that *LPP3* is essential to formation of the chorio-allantoic placenta and extra-embryonic vasculature. *LPP3* also mediates gastrulation and axis formation, probably by influencing the canonical *Wnt* signaling pathway. The exact biochemical roles of LPP3 phosphatase activity and its undefined effect on β-catenin-mediated TCF transcription remain to be determined.

Key words: Lipid phosphate phosphatase, Vasculogenesis, Wnt, Axis duplication

Introduction

Interactions between cells are central to normal embryonic development. Signal transduction pathways governing differentiation, pattern formation, migration and morphogenesis of cells within embryos are conserved across species. However, analysis of such interactions has largely focused on the roles of polypeptide growth factors binding to specific transmembrane receptors. Increasingly, it is becoming apparent that bioactive lipids generated from membrane phospholipids are also potent mediators of a variety of cellular functions. Phospholipids and their derivatives, such as sphingosine-1-phosphate (S1P), lysophosphatidic acid (LPA) and ceramide affect a broad spectrum of cellular processes including, proliferation, apoptosis, differentiation, chemotaxis, adhesion and secretion (Goetzl and An, 1998; Liu et al., 1999).

Bioactive phospholipids are synthesized and degraded by a complex set of metabolic pathways. In adult mammals they are present at nano- to micromolar concentrations in serum with their principal source being activated platelets and cells stimulated by growth factors and cytokines (Yatomi et al., 1997). The phospholipids, S1P and LPA, act on cells by binding to the S1P and LPA receptors [formerly the Edg receptors (Chun et al., 2002)], G protein coupled trans-membrane receptors (Fukushima and Chun, 2001; Hla, 2001). Activation of these receptors enhances adhesion, migration and morphogenesis of capillary endothelial cells, as well as inhibiting T-cell apoptosis. However, the mitogenic effects of phospholipids on other cell types may also be mediated by their action as intracellular second messengers, although they may also be acting through other, as yet unidentified, receptors.

Given their effects on cells, recent evidence has revealed that these lipid mediators are important to embryogenesis, particularly in guiding cell migration. This was first shown by the demonstration that the products of the *Drosophila* genes *wunen* and *wunen2*, are lipid phosphate phosphatases regulating germ cell migration during development (Starz-Gaiano et al., 2001; Zhang et al., 1997). In zebrafish, the mutation *miles apart* results in a failure of the heart primordia to migrate to the midline and subsequently fuse. The altered gene encodes a protein with high homology to the

lysosphingolipid receptor $S1P_2$ (Kupperman et al., 2000). In mice, mutations in some of the S1P receptors, affect development, with $S1P_1$ deficiency resulting in mid-gestational hemorrhage and lethality due to an inability of vascular endothelial smooth muscle precursor cells to surround the blood vessels. LPA_1 deficiency caused a high frequency of perinatal lethality, postnatal growth defects and a low incidence of hematomas (Contos et al., 2000; Liu et al., 2000). Null mutations in other S1P and LPA receptors including $S1P_2$ and $S1P_3$ and LPA_2 had little overt effect, indicating considerable redundancy between the receptors (Contos et al., 2002; Ishii et al., 2002). Nevertheless, these results suggests that a strict regulation of the levels of lipid phosphates during development are required to properly control cellular responses to these molecules.

The lipid phosphate phosphatases (LPPs) are a group of enzymes involved both in lipid phosphate biosynthesis and maintaining the balance between bioactive phosphorylated and dephosphorylated forms (Sciorra and Morris, 2002). The LPPs are glycoproteins with a channel-like structure containing six putative transmembrane domains (Kanoh et al., 1997) and were first characterized from their ability to dephosphorylate phosphatidic acid (PA) to produce diacylglycerol (DAG). Since PA and DAG act as potent signaling molecules, LPPs play a key role in signal transduction in addition to regulating lipid biosynthesis. Two classes of mammalian LPPs have been identified. The type 1 (LPP1) is a cytoplasmic, Mg^{2+}-dependent enzyme, sensitive to N-ethylmaleimide and is required for glycerolipid biosynthesis. The type 2 LPPs, are membrane bound enzymes, Mg^{2+}-independent and N-ethylmaleimide-insensitive and are involved in signal transduction mediated by phospholipase D (Sciorra and Morris, 2002). In humans, at least three genes coding for type 2 LPP enzymes have been identified (*LPP1*, *LPP2* and *LPP3*) (Kai et al., 1997; Roberts et al., 1998). In addition to PA, all LPPs hydrolyze LPA, ceramide-1-phosphate (C-1-P) and S1P (Kai et al., 1997; Roberts et al., 1998). Of the three LPPs, *LPP3* has unique characteristics: it localizes to both the plasma membrane and intracellular organelles depending on cell type (Sciorra and Morris, 1999) and its transcription is stimulated by epidermal growth factor (Kai et al., 1997). *LPP3* corresponds to the previously identified gene product of *Dri42* from rat (Barila et al., 1996) that is upregulated during intestinal epithelial differentiation.

Apart from the role of *wunen* in regulating *Drosophila* germ cell migration, and left-right asymmetry in the gut (Ligoxygakis et al., 2001), little is known about the role of these signal modulators in development. Because of the increasing evidence of phospholipids influencing both cellular morphology and locomotion we investigated the expression and functions of the murine LPP (*Ppap* – Mouse Genome Informatics) homologues in development. We report that *LPP3* exhibits a highly tissue-specific and dynamic pattern of expression during post-implantation development in contrast to both *LPP1* and *LPP2*, which are more uniformly and widely expressed. To analyze the role of *LPP3* in development we introduced a deletion into the *LPP3* locus. This mutation revealed that the enzyme is essential for development of the allantoic and yolk sac vasculature, as well as the chorio-allantoic placenta. In addition a subset of embryos exhibited profound alterations in axis formation that were similar to mutations associated with *axin* deficiency (Zeng et al., 1997). The latter phenotype is associated with alterations to the Wnt signaling pathways. We show that transcriptional activity of the TCF co-factor β-catenin is regulated by a previously unidentified function of LPP3 that is independent of its lipid phosphatase activity.

Materials and methods

Generation of *LPP3*-deficient ES cells and mice

The mouse EST AA276423 [I.M.A.G.E. Consortium clone ID 776179 (Lennon, 1996)] was used to screen a 129/SvJ mouse genomic BAC library (Research Genetics). From the clone BJ4123, a 4 kb *Hin*dIII fragment with the exon coding for the third outer loop of *LPP3* was used to produce a replacement targeting vector containing *PGKneo* and *TK* cassettes for positive and negative selection, respectively. W9.5 ES cells were electroporated with the targeting construct and 2 homologous recombinant clones (12-2B4 and 43-1F3) were microinjected into C57BL/6J blastocysts. Chimeras from both cell lines transmitted the mutated allele through the germline and were used to establish the mouse lines.

Genotyping of mouse embryos by PCR

The extra-embryonic membranes were analyzed by PCR (lysis buffer 50 mM KCl, 10 mM Tris pH 8.3, 2 mM $MgCl_2$, 0.01% gelatin, 0.45% NP-40, 0.45% Tween 20, 100 μg/ml of proteinase K). Embryos were genotyped using a set of three oligonucleotides distinguishing the wild type and mutant alleles. Wild type: 5′-gccttctacacgggattgtcac-3′; mutant PGK forward: 5′-cagaaagcgaaggaacaaagctg-3′; common reverse: 5′-ttgtgctcacagagaaggaggattc-3′. The PCR products obtained after 30 cycles yielded fragments with the following sizes: wild type allele 302 bp and mutant allele 500 bp.

Derivation of homozygous mutant ES cells, embryoid bodies and production of ES cell-derived embryos

ES cell lines were established from blastocysts of heterozygous intercrosses as described previously (Abbondanzo et al., 1993). The genotype of each clone was verified by Southern blot hybridization and lines with a normal diploid karyotype were identified. Embryoid bodies were prepared from ES cell lines essentially as described (Robertson, 1987). ROSA26 blastocysts (Zambrowicz et al., 1997) were injected with homozygous mutant $LPP3^{StwO3}$ ES cells. Embryos were recovered from equivalent 9.5 to 10.5 days of gestation. β-galactosidase staining was performed to reveal the contribution of wild-type and mutant cells to the conceptuses.

Whole-mount in situ hybridization

Mouse embryos were fixed and processed for in situ hybridization as described previously (Hogan, 1994). Antisense RNA probes for *brachyury*, *Shh*, *Twist*, *flk1*, *hex*, *wnt3*, *LPP1* (I.M.A.G.E. Consortium Id clone 732307) and *LPP2* (I.M.A.G.E. Consortium Id clone 766619) were utilized. Frog embryos whole-mount in situ hybridization was done essentially as described by Harlan (Harlan, 1991) using riboprobes for *Xpax6*, *Xotx2*, *Xkrox20*.

β-galactosidase staining

Embryos were stained as described previously (Hogan, 1994). Embryos were immersed for 15-30 minutes in fixative solution (0.2% glutaraldehyde, 5 mM EGTA, 2 mM $MgCl_2$ in PBS), washed 3 times 30 minutes with detergent rinse (2 mM $MgCl_2$, 0.02% NP-40, 0.01% sodium deoxycholate in PBS) and incubated overnight at 37°C in staining solution (2 mM $MgCl_2$, 0.01% sodium deoxycholate, 0.02% NP-40, 5 mM potassium ferricyanide, 5 mM potassium ferrocyanide, X-gal 1 mg/ml). When necessary embryos were embedded in paraffin, sectioned at 7 μm and counterstained with Fast Red.

Histology

Tissues were fixed with 4% paraformaldehyde in PBS overnight, ethanol dehydrated and embedded in wax. 7 μm thick sections were stained with Hematoxylin and Eosin. For high resolution microscopy embryos were immersed in Karnovsky's fixative solution (3% glutaraldehyde, 1% paraformaldehyde in 0.1 M sodium cacodilate buffer, pH 7.4), postfixed with 1% OsO_4, ethanol dehydrated and embedded in epon 812. Semithin sections (1 μm) were stained with Toluidine Blue.

Immunohistochemistry

Detection of endothelia in allantois cultures

After culture, explants were fixed for 15 minutes with 4% paraformaldehyde in PBS and blocked with PBSMT (2% skim milk, 0.5% Tween in PBS), samples were incubated overnight with 10 μg/ml of anti-mouse PECAM1 antibody (Pharmingen, MEC13.3) at 4°C followed by 6 washes for 1 hour each in PBSMT and overnight incubation with 1:100 anti-rat HRP-coupled antibody at 4°C. After an additional round of washes color reaction was performed in the presence of DAB and H_2O_2.

PECAM1 whole-mount immunohistochemistry

Embryos were treated essentially as described previously (Schlaeger et al., 1995). Antibody was used at the same concentration as for immunohistochemistry.

Frog embryo injections

PCR generated full-length mRNAs of murine *LPP3* and *LPP3* with a deletion of amino acids 187-219, containing the third outer loop, were cloned into the pCS+ vector. *Xenopus* embryos were microinjected with mRNA derived from *Not*I-linearized constructs transcribed with the mMessage mMachine kit (Ambion). 2.5 ng of *LPP3* RNA were coinjected with 1.15 and 0.46 pg of *Xwnt3a* and *Xwnt8* RNA, respectively, into the two ventral blastomeres of four-cell embryos.

Western blot

Cells or tissues were lysed with 50 mM Tris pH 8.0, 150 mM NaCl, 1% NP-40, 1× complete protease inhibitor cocktail (Roche). 50 μg of protein were run in denaturing acrylamide gels and transferred to PVDF membranes. Antibodies were to phospho-pan PKC (Cell Signaling, 9371), Anti-active β-catenin (anti-ABC) (Upstate Biotechnology) LPP3 (Sciorra and Morris, 1999), actin (Santa Cruz), phospho-GSK3-β (Ser-9) (Cell Signaling, 9336S), GSK-3 (Transduction Laboratories, G22320). Protein was detected using the ECL-plus system (Amersham).

Cell culture

MEFs were derived from wild type and wild type↔*LPP3*$^{-/-}$ E13 chimeras. Embryos were isolated, heart and livers removed and then rinsed with PBS, minced, and digested in 2 ml DMEM containing 100 μg/ml DNaseI and collagenase IV (Sigma) for 30 minutes at 37°C. The cells were pelleted and resuspended in DMEM-10% FBS and the mutant cells isolated by culturing in the presence of 500 μg/ml G418. The purity of mutant cells was confirmed by PCR genotyping.

Transient transfection and luciferase reporter assays

HEK293 cells were from the American Type Culture Collection. W9.5 and LPP3$^{-/-}$ ES cell lines (described above) were grown under feeder-free conditions (Abbondanzo et al., 1993). 1×10^5 cells were co-transfected using Fugene 6 (Roche) with 2 μg of Renilla luciferase internal standard pRLCMV (Promega), and/or TOPFlash or FOPFlash firefly luciferase reporter plasmid (Upstate Biotechnology) with β-catenin (human full-length cDNA in pcDNA3.1; courtesy of T. Yamaguchi) or mutant β-catenin (dominant active, containing deleted Gsk3β recognition sites in pcDNA3.1; courtesy of T. Yamaguchi) and full-length or mutant *LPP3*cDNA in pIRES-hrGFP-1a. pcDNA3.1 (In Vitrogen) plasmid was added to standardize DNA quantities. After 48 hours, luciferase activity was determined using the Dual-Luciferase assay system (Promega) as described by the manufacturer.

Measurement of phosphatidic acid levels

Wild-type and *LPP3*$^{-/-}$ cells (2×10^6) were seeded in 100 mm plates. One day later, the cells were incubated with 5 μCi/ml of [^{3}H]palmitic acid for 24 hours. Lipids were extracted essentially as previously described with a minor modification (Zhang et al., 1991). Briefly, cells were scraped in 2×600 μl methanol/HCl (200:2). The extracts were sonicated and 600 μl of chloroform was added followed by 500 μl of H_2O, and phases separated by addition of 600 μl of 2 M KCl and 600 μl of chloroform, followed by vortexing and centrifugation. An aliquot of the organic phase containing 10×10^6 cpm was spotted on silica gel plates. The plates were developed in the organic phase of a mixture of ethyl acetate/2,2,4-trimethylpentane/acetic acid/H_2O (13:2:3:10). The products were revealed by autoradiography and identified by co-migration with standards. The individual phospholipids were scraped from TLC plates and radioactivity quantified by liquid scintillation.

Measurement of monoacylglycerol and diacylglycerol levels

Diacylglycerol and monoacylglyerol in cellular extracts were measured by the diacylglycerol kinase enzymatic method (Olivera et al., 1997). Briefly, aliquots (10-50 nmol of total phospholipid) of the chloroform phases from cellular lipid extracts were resuspended in 40 μl of 7.5% (w/v) octyl-β-D-glucopyranoside/5 mM cardiolipin in 1 mM DETPAC/10 mM imidazole (pH 6.6) and solubilized by freeze-thawing and subsequent sonication. The enzymatic reaction was started by the addition of 20 μl DTT (20 mM), 10 μl *E. coli* diacylglycerol kinase (0.88 U/ml), 20 μl [γ-^{32}P]ATP (10-20 μCi, 10 mM) and 100 μl reaction buffer (100 mM imidazole (pH 6.6), 100 mM NaCl, 25 mM $MgCl_2$, and 2 mM EGTA). After incubation for 1 hour at room temperature, lipids were extracted with 1 ml chloroform/methanol/HCl (100:100:1, v/v) and 0.17 ml of 1 M KCl. Labeled phosphatidic acid and lysophosphatidic acid were resolved by TLC with chloroform/acetone/methanol/acetic acid/water (10:4:3:2:1, v/v) and quantified with a Molecular Dynamics Storm phosphorimager. Known amounts of diacylglycerol and monoacylglycerol standards were included with each assay.

Analysis of labeled phospholipids released by MEFs

Wild-type and *LPP3*$^{-/-}$ cells (2×10^6) were seeded on 100 mm plate. One day later, the cells were incubated with 40 mCi/ml of [^{32}P]Pi for 24 hours. Lipids in the extracellular medium were extracted (Bligh and Dyer, 1959). Briefly, 2 ml of medium were extracted with 5.4 ml of methanol/$CHCl_3$/HCl (100/200/2). Then, 2.4 ml of 2 M KCl and 2.4 ml of $CHCl_3$ were added. After phase separation, the organic layer was dried under nitrogen and dissolved in $CHCl_3$/methanol (3:1). Lipids were separated by TLC using $CHCl_3$/acetone/methanol/acetic acid/water (5/4/3/2/1). Labeled lipids were detected and quantified using a PhosphoImager (Image Quant software, Molecular Dynamics) and data expressed as fold increase normalized to the total amount of phospholipids. [^{32}P]LPA was identified by co-migration with unlabeled LPA.

Results

Expression of *LPPs* during early development

A detailed analysis on the expression pattern of the individual murine *LPP* genes, in early development, was performed by whole-mount in situ hybridization with probes specific for the three known members of this gene family. *LPP1* is constitutively expressed throughout development and present

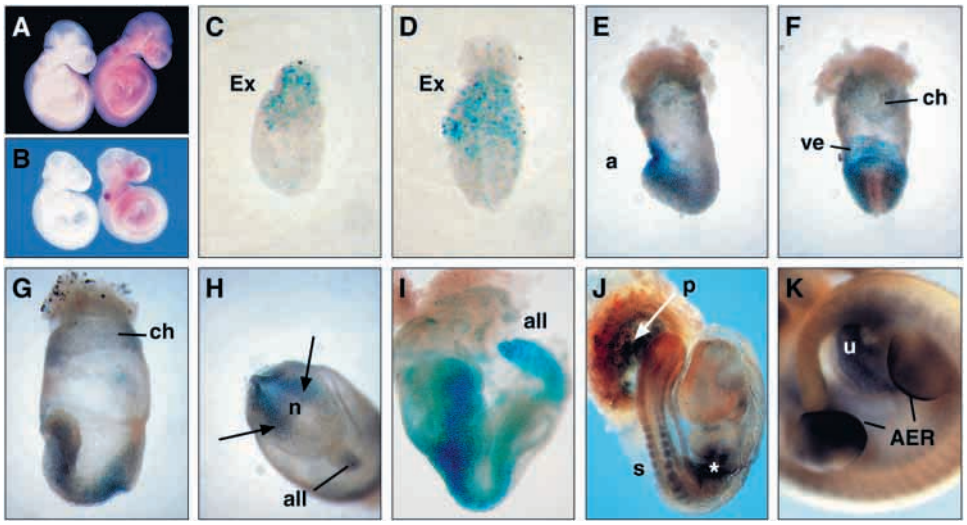

Fig. 1. Embryonic expression pattern of *LPP* genes. *LPP1* in situ hybridization in an E9.5 embryo (left sense, right antisense) with a uniform ubiquitous expression (purple color). (B) *LPP2* in situ hybridization in an E9.5 embryo (left sense, right antisense). *LPP2* is weakly but still widely expressed (purple color). (C-K) *LPP3* expression in *LPP3-IRESlacZ* embryos as revealed by β-galactosidase staining (blue). (C,D) E6.5 embryos showing expression in the extra-embryonic ectoderm (Ex). (E,F) In E7.5 embryos *LPP3* is expressed in the anterior (a) domain of the embryo and extra-embryonic membranes. (E) lateral and (F) frontal views. ve, visceral endoderm; ch, chorion. (G,H) E8.0 embryo showing expression of *LPP3* in (G) the chorion and anterior domain of the embryo and (H) around (arrows) the node (n) and in the tip of the allantois (all). (I) E8.5 embryo showing strong *LPP3* expression in the allantois (all) and paraxial mesoderm. (J) E9.5 embryo showing expression in the somites (s), developing gut (*) and the chorio-allantoic placenta (p). (K) E10.5 embryo showing *LPP3* expression in the limb with strongest expression in the apical ectodermal ridge (AER) and continued expression in the umbilical cord (u).

in all tissues in midgestation embryos, whereas *LPP2* has a diffuse but more restricted pattern of expression (Fig. 1A,B and data not shown). The expression of *LPP3* during embryogenesis was determined by a combination of mRNA whole-mount in situ hybridization, antibody staining to LPP3 protein and reporter analysis following insertion of the bacterial *lacZ* gene into the *LPP3* locus (see below). The *LPP3-IRESlacZ* allele bicistronically expresses a truncated LPP3 transcript fused to *lacZ* (unpublished data) thereby localizing endogenous LPP3 transcripts by the activity of β-galactosidase (β-gal).

In contrast to the uniform expression of the other LPPs, *LPP3* is expressed during postimplantation development in a dynamic fashion (Fig. 1C-K). β-gal expression is first detected in a few cells of the extra-embryonic ectoderm of E6.5 embryos (day of plug≡day 0.5) (Fig. 1C,D). The position of the extra embryonic ectoderm in these stages was confirmed by sectioning the stained embryos (data not shown). By E7.5, *LPP3* starts to be strongly expressed in the anterior visceral endoderm, as well as in the extra-embryonic membranes (Fig. 1E,F). By E8.0 expression extends to a highly localized region around the node and appears at the tip of the allantois (Fig. 1G,H). At E8.5 *LPP3* is predominantly expressed in the allantois, the developing gut, the pericardio-peritoneal canal and somites (Fig. 1I). *LPP3* in E9.5 embryos persists in the umbilical cord, and is also found in the chorionic region, probably because of the contribution by the allantois to the chorio-allantoic placenta (before fusion, the chorion exhibits low levels of *LPP3*) (Fig. 1J). In later mid-gestation embryos *LPP3* is present at high levels in the apical ectodermal ridge and mesenchyme of the limb buds (Fig. 1K), in the peripheral nervous system, cranial nerves, and mammary gland primordia (not shown). In adults significant levels of *LPP3* mRNA were localized to the lung, cerebellum and heart atrium (data not shown), revealing a dynamic and changing pattern of expression throughout the life cycle of the mouse.

Derivation of mice lacking *LPP3* activity

To establish whether *LPP3* is required during development, we inactivated the gene by targeted mutagenesis. A replacement-type targeting vector was used in which a *PGKneo* cassette, flanked by *loxP* sites (floxed), was introduced so that after recombination, the exon coding for amino acids 214-268 of the protein, containing part of the presumptive catalytic domain (Fig. 2A), was eliminated. Deletion of this region removes part of the fourth, fifth and sixth transmembrane domains, as well as the second internal loop and third outer loop of the protein. ES clones heterozygous for the mutated allele were derived (13/149) (Fig. 2B) and 2 independent lines of mice (12.2B4 and 43.1F3) were established by blastocyst injection. Both lines showed the same phenotypic characteristics (see below). This allele is referred to as $LPP3^{StwO3}$.

Northern analysis on embryoid bodies (EBs) derived from differentiated heterozygous and homozygous *LPP3* mutant ES cell lines showed that although a transcript was still present, it was smaller (Fig. 2D). However western analysis on primary fibroblast lines derived from the embryos demonstrated a reduction in LPP3 protein levels in the heterozygous cells and a complete absence of intact protein in the homozygous lines (Fig. 2E). Using an antibody against LPP3 (Sciorra and Morris, 1999), protein immunoprecipitated from cultured heterozygous EBs produced DAG from PA with a mean activity of 21.5 pmol/minute. In contrast LPP3 from homozygous EBs was unable to do so (mean activity 0.6 pmol/minute) showing that the $LPP3^{StwO3}$ mutation in the homozygous state abolished LPP3 phosphatase activity. Subsequently, we utilized wild-type and *LPP3* homozygous mutant mouse embryonic fibroblasts (MEFs) to determine changes in other intracellular phospholipids. Homozygous $LPP3^{StwO3}$ MEFs had an almost 50% reduction in the levels of DAG compared to wild types, whereas the levels of monoacylglycerol (MAG), were not significantly changed (Table 1). Because the amount of PA is less than 1% of the total phospholipids, it is difficult to

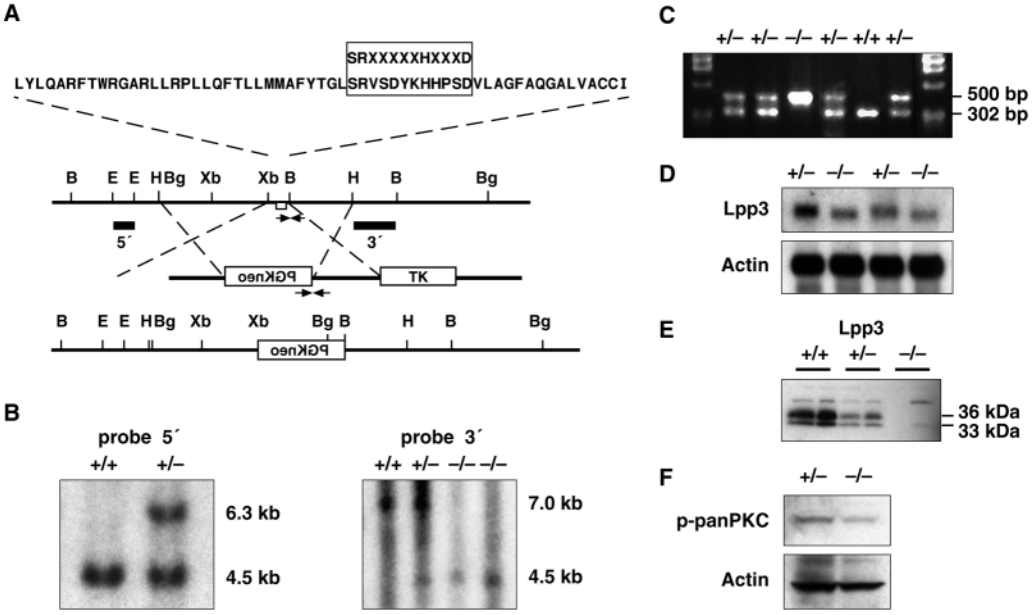

Fig. 2. Inactivation of *LPP3* by homologous recombination in ES cells. (A) Gene targeting strategy. The exon containing the 3rd outer loop, containing part of the catalytic domain (box), was deleted (top). The structure of the wild-type allele (middle) and targeted allele (bottom) after homologous recombination are shown. The fragments used for confirming 5′ and 3′ recombination as well as the location of the primers used for PCR genotyping (arrows) are indicated. (B) *LPP3* genotyping by Southern blot. *Bam*HI *and Bgl*I digested DNAs were tested with 5′ and 3′ probes respectively. (C) Genotype of embryos by PCR. DNA samples of yolk sacs were used for amplification of mutant and wild-type allele products using the set of 3 primers indicated in A. Wild-type product = 302 bp; mutant product = 500 bp. (D) Northern blot of embryoid body (EBs) total RNA shows the presence of a smaller transcript (–177 bp) in homozygous mutant cells resulting from the deletion of the exon. (E) Western blot of primary cultured cells revealed a reduction in the levels of LPP3 in heterozygous cells (compare to wild-type) and the absence of any intact protein in homozygous mutant cells. The 36 kDa upper band corresponds to the glycosylated form of the enzyme. (F) PKC phosphorylation in heterozygous and homozygous mutant EBs cultured for 12 days. A phospho (pan)-PKC antibody was used to indirectly measure PKC activation. A reduction of around 50% phospho-pan PKC was observed in the homozygous compared with the heterozygous tissues. Actin was used as a control for amount of protein loaded.

Table 1. Phospholipids in wild-type and *LPP3*$^{-/-}$ mouse embryonic fibroblasts

Lipids	Wild type	*LPP3*$^{-/-}$
DAG (pmol/nmol phospholipid)	15.1±1.7	8.3±0.6
MAG (pmol/nmol phospholipid)	6.6±1.1	5.4±2.8
% PA	0.64	0.90
% unknown	1.08	2.15
Extracellular LPA (pmol/nmol of phospholipids/ml)	1.85±0.07	4.7±0.09

MAG, monoacylglycerol; DAG, diacylglycerol; PA, phosphatidic acid; LPA, lysophosphatidic acid. Values are mean±s.e.m.

There were no significant differences in the major phospholipids phosphatidylcholine (PC) and phosphatidylethanolamine (PE). Percentage PC and PE in wild-type and KO MEFs were 83.2±2.0 (for PC) and 14.4±2 (for PE), respectively.

accurately measure small changes in mass. To determine changes in PA levels, cells were labeled with [^{3}H]palmitic acid to enhance the sensitivity of detection. This revealed that PA was a minor component compared to other phospholipids, including phosphatidylcholine and phosphatidylethanolamine. Two-dimensional TLC analysis did not reveal any significant changes in the major phospholipids present in the mutant MEFs compared to wild-type cells with intracellular LPA and S1P being undetectable in both (data not shown). There was a small but significant increase of PA in the *LPP3*$^{-/-}$ cells compared to wild type (Table 1). In addition, there was an increase in an unidentified phospholipid that migrated slightly faster than PA (Table 1). These data indicate that the lack of LPP3 activity results in, as expected, a decreased level of DAG and concomitant increase in PA. Since DAG induces the phosphorylation of several isoforms of PKC, resulting in their activation, we determined the levels of phosphorylated PKC. Homozygous null EBs showed approximately 50% lower phospho-pan PKC than their heterozygous counterparts (Fig. 2F).

To examine if extracellular phospholipid levels were altered by the lack of LPP3 activity, ^{32}P-labeled lipids were extracted from the culture medium of wild- type and *LPP3*$^{-/-}$ MEFs. Medium from null MEFs had a 2.6 fold increase in the levels of LPA over that of wild type (Table 1) indicating an extracellular accumulation of this phospholipid, whereas S1P was undetectable.

Together these results reveal that the targeted mutation deleting *LPP3*, resulted in an increase of both extracellular LPA and intracellular PA, as well as a significant reduction in the intracellular levels of DAG, concomitant with a reduction in the levels of activated PKC.

Absence of LPP3 results in embryonic lethality and is associated with two post-implantation phenotypes

Heterozygous *LPP3*^{StwO3} mice were viable, fertile and indistinguishable from their wild-type littermates. Matings of heterozygous *LPP3*^{StwO3} on either a mixed 129/SvJ×C57BL/6J or a pure 129/SvJ background produced animals only of wild-type and heterozygous genotype (Table 2), indicating that the mutation is an embryonic lethal. Embryos from *LPP3*^{StwO3} heterozygous intercrosses were analyzed at 7-10.5 days of gestation and genotyped by PCR (Fig. 2C). In these, a normal

Table 2. Distribution of genotypes in newborn mice and embryos from *LPP3^{StwO3}* heterozygous intercrosses (mix background)

Genotype	E7.5 *n*(%)	E8.5 *n*(%)	E9.5 *n*(%)	E10.5 *n*(%)	Born *n*(%)
Wild type	11 (24)	21 (23)	24 (23)	6 (20)	72 (26)
Heterozygous	22 (48)	55 (60)	50 (48)	14 (48)	202 (74)
Homozygous	13 (28)*	16 (17)*	**29 (28)***	**9 (31)**	0 (0)

*31% of the embryos had axis duplication or were highly abnormal.
Bold, embryos reaching these stages also lacked a chorio-allantoic placenta, with an abnormal allantois and were developmentally delayed.

Mendelian distribution of genotypes was observed (Table 2). No live homozygous embryo was recovered beyond E10.5 indicating embryonic lethality prior to or around this time. Homozygous embryos collected between E7-10.5 were, in general, developmentally delayed when compared to wild-type or heterozygous littermates. Moreover, 30% of the homozygous mutant embryos were highly abnormal revealing a gastrulation defect (see below).

During normal embryogenesis, around E8.5-9 (or 6-somite stage), the embryo turns and the allantois and chorion fuse to form the chorio-allantoic placenta. In contrast *LPP3^{StwO3}* homozygous embryos were developmentally delayed by 12-24 hours (Fig. 3A-D). Mutant embryos at E9.5-10.5 with 6 or more somite pairs invariably had an abnormal allantois that did not connect with the chorionic plate (Fig. 3D,E). The allantois, instead of extending from the embryo towards the chorion, was compacted and curled over the embryo and amnion (Fig. 3D). In the few E10.5 homozygous mutant embryos with more advanced development, the allantoises remained as a compact mass of tissue, in which erythropoiesis and vasculogenesis was evident, but the allantoises still did not contact the chorion (Fig. 3E-F).

The mutant embryos recovered at E9.5-10.5 also exhibited abnormal vascularization of the yolk sac (Fig. 4A). While the yolk sac of wild-type and heterozygous embryos had a vascular plexus (Fig. 4B,C), yolk sacs from null embryos were pale and translucent, with limited formation of a vascular network (Fig. 4E,F) with frequent accumulation of blood cells in the yolk sac cavity. Staining for *flk1* (a marker for capillary endothelial

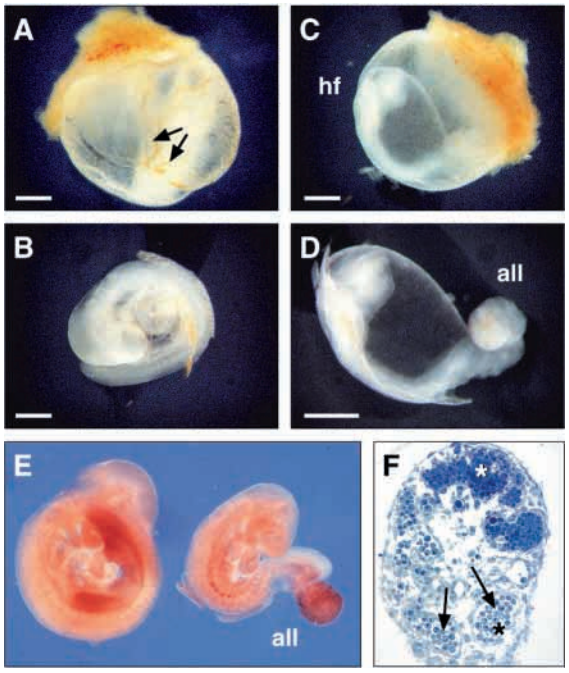

Fig. 3. Phenotype of *LPP3*-deficient embryos. (A,B) E9.5 wild-type embryo showing the vascularization of the yolk sac (A, arrows), and normal embryonic development at this stage (B); the embryo has turned and the allantois has contacted the chorion. In this individual the connection was lost because of the removal of the extra-embryonic membranes. (C,D) E9.5 homozygous null sibling of the embryo shown in (A,B). The extra-embryonic membranes appear thin, pale, with an anemic appearance and no indication of large blood vessel formation (C). The embryo was smaller and developmentally delayed. The most evident malformation is the abnormal development of the allantois (all). (E) A unique *LPP3$^{-/-}$* embryo (right) recovered at E10 showing an advanced developmental progression. Despite an almost normal appearance, the allantois (all) of this embryo formed a very compact mass of tissue. The differentiation of allantoic endothelial cells was demonstrated by the presence of the endothelial marker flk-1 (brown staining). A heterozygous sibling is shown on the left. (F) Semithin section through the allantois of an E9.5 mutant embryo showing blood vessels formation (arrows) and differentiation of hematopoietic cells (asterisk). Scale bars, 0.5 mm.

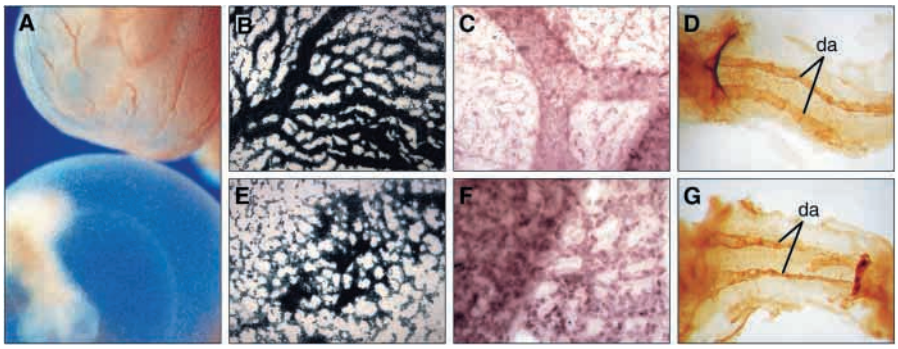

Fig. 4. *LPP3$^{-/-}$* yolk sacs show abnormal vasculogenesis. (A) External appearance of the yolksac in normal (top) and homozygous mutant (bottom) conceptuses recovered at E10.5. In the mutant note the complete absence of blood vessels and a very delayed embryo with its corresponding amnion that can be observed through the yolk sac. (B,C) Development of the vascular plexus in an E10.5 wild-type yolk sac. Formation and ramification of large blood vessels is evident when blood cells are detected by their endogenous peroxidase activity (B) or by staining endothelial cells using a *flk-1* probe (C). (D) PECAM-1 detection of endothelial cells in a wild-type mouse embryo at E8.5 showing the formation of the dorsal aortas. (E,F) An E10.5 *LPP3$^{-/-}$* yolk sac showing a poor development of the vascular plexus. No large blood vessels were formed. Blood cells and endothelial cells were detected as in B and C. (G) PECAM-1 detection of endothelial cells in a *LPP3-deficient* embryo at E9.5 showing the formation of the dorsal aortas.

cells) in the mutant yolk sacs revealed that endothelial cells were present but had failed to organize into a capillary network (Fig. 4C,F). Although hemorrhaging of the *LPP3*-deficient embryos was frequently observed, development of the internal embryonic vasculature appeared to be overtly normal with the major embryonic vessels such as the dorsal aortas being identifiable by anti PECAM1 staining (Fig. 4D,G).

These results reveal that LPP3 is essential to normal mouse embryogenesis during the first days of post-implantation development. A generalized developmental delay, presumably due to abnormal morphogenesis of the yolk sac vasculature and the failure to establish a chorio-allantoic placenta were considered to be the principal embryonic defects leading to lethality.

Disruption of allantois morphogenesis leads to defective placenta formation

To gain further insight into the placental phenotype, we analyzed the developmental potential of *LPP3* null cells in chimeric combination with wild-type embryos. Homozygous *LPP3*^{StwO3} ES cells were injected into wild-type ROSA26 blastocysts constitutively expressing the *lacZ* reporter gene. Under these conditions, extra-embryonic tissues, including the chorion, will be of wild-type genotype with the mutant ES cells contributing to both the embryonic and extra-embryonic mesoderm. In the presence of wild-type extra-embryonic tissue, allantoises from embryos entirely derived from the null ES cells (n=3) were able to contact the wild-type chorion (Fig. 5A). Histological analysis of the chorio-allantoic region revealed that despite contact between both structures, the allantois remained as a compact mass of tissue that did not extensively invade the chorionic plate (Fig. 5C). The vascular adhesion molecule 1 (VCAM1) and its receptor, α4 integrin, are both required for chorio-allantoic fusion. Embryos lacking VCAM1 in the allantois or α4 integrin in the chorion fail to establish a proper chorio-allantoic connection (Gurtner et al., 1995; Yang et al., 1995). A comparison between heterozygous and homozygous mutant embryos, at equivalent stages of development (5-6 somite pairs), revealed no significant differences in the expression or tissue distribution of VCAM1 and α4 integrin between embryos of both genotypes (data not shown). This indicated that additional and as yet unidentified cellular components are involved in chorio-allantoic fusion, and are affected by LPP3 deficiency. In the chimeras, with contributions from both wild-type and mutant cells to the embryo proper, chorio-allantoic placental and vascular development was much improved, however the majority of allantoic endothelial cells were of wild-type origin (Fig. 5B,D). These observations reveal that *LPP3* is required, both in the chorion to promote allantois extension and fusion with the chorion, and also in the allantois to enable it to undergo proper vasculogenesis.

To test this, we cultured wild-type and homozygous mutant allantois isolated from embryos at the 4-5 somite stage, and analyzed their growth and differentiation in vitro. Twenty-four to 36 hours after explanting the allantoises, those that were wild-type or heterozygous had spread over the culture surface and developed a network of long, thin capillary-like structures. Staining with anti-PECAM1 antibodies revealed the network was composed of endothelial cells (Fig. 5E). In contrast, in the homozygous mutant allantoises, both the mesothelial and mesenchymal tissues spread over the culture surface, but a compact mass of PECAM1-positive tissue occupied the center of the explant, with no evident capillary or cord formation (Fig. 5F). An identical effect on capillary formation, was also produced by culturing wild-type allantoises in the presence of 75 μM propranolol, a potent inhibitor of LPP activity (Pappu and Hauser, 1983) (data not shown).

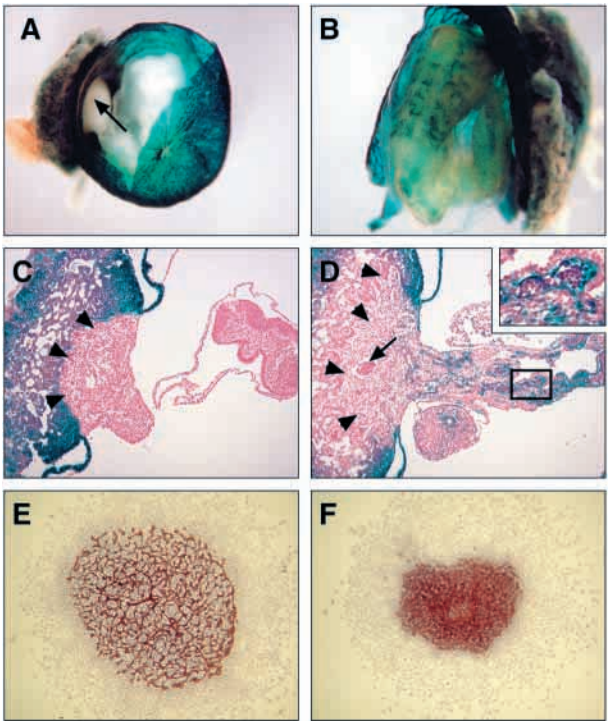

Fig. 5. Extra-embryonic expression of LPP3 partially rescues the placental phenotype and reveals abnormal allantoic vasculogenesis. (A) *Rosa26*↔*LPP3*$^{-/-}$ chimeric embryo recovered at E10.5. In the presence of wild-type extra-embryonic tissue (blue), the allantois from this embryo, entirely derived from *LPP3*$^{-/-}$ cells, contacted the chorion (arrow). The embryo is also developmentally delayed. (B) *Rosa26*↔*LPP3*$^{-/-}$ chimeric embryo recovered at E10.5. This embryo, formed by a mixture of wild-type (blue) and mutant cells showed more advanced development. Compare with the size and stage of development of the littermate embryo shown in A. The allantois also contacted the chorion (not shown). (C) Transverse section through the chorio-allantoic region of the embryo shown in A. The section corresponded to the maximum diameter of the chorio-allantoic region. Although *LPP*$^{-/-}$ mutant cells (pink) contacted the chorion (arrowheads), the allantois remained as a compact mass of tissue that did not invade the chorion. (D) Transverse section through the chorio-allantoic region of the mixed chimera shown in B. Chorio-allantoic placental development was enhanced in the presence of a mixed population of *LPP*$^{+/+}$ (blue) and *LPP*$^{-/-}$ cells. Chorionic development was enhanced, as shown by the wavy appearance of the chorion (arrowheads), increased diameter of the placenta and the formation of large allantoic blood vessels (arrow). Note that the endothelial cells from the umbilical cord vessels were predominantly of wild-type genotype (inset, blue cells). (E) Allantois from a 5-somite wild-type embryo cultured for 36 hours. Note that the PECAM1 positive endothelial cells (brown) developed a flat network of thin capillary-like structures. (F) Allantois from a 5-somite *LPP3*$^{-/-}$ embryo treated as in E. A mass of PECAM1-positive endothelial cells remained in the center of the explant.

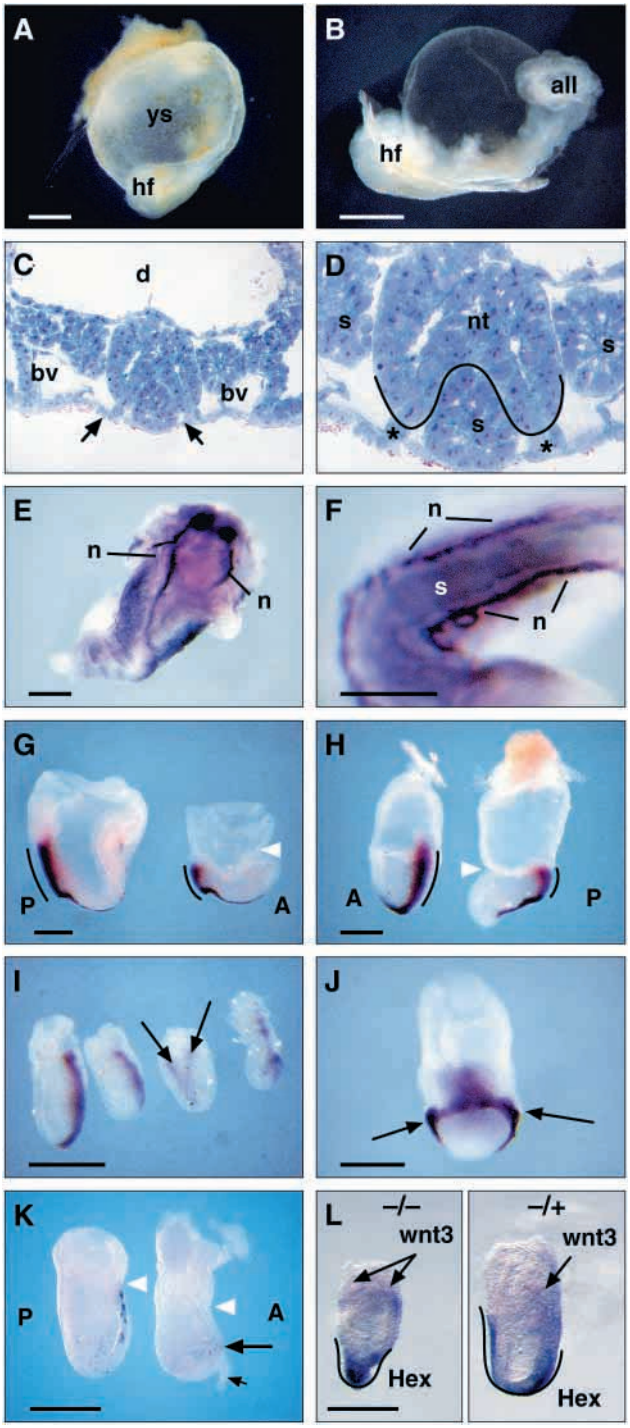

Fig. 6. *LPP3* deficiency results in axis duplication. (A,B) An E9.5 *LPP3*$^{-/-}$conceptus where the anterior part (hf) of the embryo developed outside the yolk sac (ys) and also exhibited abnormal vasculogenesis (A). When dissected from the extra-embryonic membranes (B), the embryo showed abnormal development of the allantois (all). (C) Cross section through an abnormal embryo showing deficiency in mesenchymal tissue around the paraxial mesoderm. Two large blood vessels (bv) have developed ventral to the somites. d, dorsal. (D) Higher magnification of C showing the neural tube (nt) clearly duplicated in the ventral region, in which a double notochord (*) is also evident. A third somite (s) row has formed ventrally to both notochords. (E,F) *Shh* and *Twist* double whole-mount in situ hybridization in *LPP3*$^{-/-}$ embryos with axis duplication. (E) In some embryos, two short *Shh*-positive notochords (n) were observed without an additional somite row forming between them. (F) In others, a clear *Twist*-positive extra somite row formed between the duplicated *Shh*-positive notochords. (G-H) At E8.5 (G) and E7.5 (H) *LPP3*$^{-/-}$ embryos (right) develop outside the yolk sac unlike the nornal littermate (left). A constriction between the embryonic and extra-embryonic tissues (arrowhead) is present. In the null embryos the *brachyury*-expressing primitive streak is shorter in the mutant embryo that in the wild type. A, anterior; P, posterior. (G) E8.5 embryos, (H) E7.5 embryos. (I) On the left, two E7.0 embryos show normal *brachyury* expression in the primitive streak. On the right, two abnormal littermates show retarded development (equivalent to E6.5), one of which shows primitive streak duplication (arrows). (J) Posterior view of a *LPP3*$^{-/-}$ embryo recovered at E8.5. *Brachyury* expression revealed the presence of a common primitive streak-like structure from which two axial mesoderm-like structures have formed. (K) *dkk1* expression in an E7.5 *LPP3* heterozygous (left) and homozygous mutant (right) embryos. While *dkk1* expression extends from the proximal AVE to the distal visceral endoderm in the heterozygous embryo, in the *LPP3* null embryo weak *dkk1* staining is restricted to a band of cells located in the distal visceral endoderm (arrow). An abnormal outgrowth of tissue formed exactly below the *dkk1* expression domain of this mutant embryo (small arrow). The arrowheads indicate the junction between the embryonic and extra-embyonic tissues. A, anterior; P, posterior. (L) *Hex* and *Wnt3* expression are also altered in E7.0 *LPP3* null embryos. *Hex*-positive cells accumulate in the distal tip of the egg cylinder and *Wnt3* expression is also found in the anterior embryonic ectoderm (arrows). In normal embryos *Hex* is expressed in the AVE and *Wnt3* is restricted to the posterior embryonic ectoderm. Bars: 250 μm.

LPP3-deficient embryos show defective gastrulation

In the mixed 129/S1×C57BL/6J background, approximately 30% of *LPP3* homozygous mutant embryos recovered between E7.5-E9.5 were highly abnormal (Table 2). The embryos exhibited a wide variety of abnormalities including a short anterior-posterior axis, anterior truncation, embryonic development outside the yolk sac membranes and frequent duplication of axial structures (Fig. 6A-B). Histological analysis of those with axial abnormalities revealed a duplicated notochord, with an extra row of somites between the notochords with partial to complete duplication of the neural tube (Fig. 6C,D). The expression of *sonic hedgehog* (*Shh*), a marker for axial mesoderm (notochord) and *Twist*, a marker of paraxial mesoderm (somites), confirmed the histological findings (Fig. 6E and F, respectively). By using a probe to *brachyury* (a marker for posterior and axial mesoderm) *LPP3*$^{-/-}$ embryos often showed a constriction between the embryonic and extra-embryonic tissues (arrowhead), with shortening of the primitive streak (Fig. 6G,H). In addition, axis duplication was detected in embryos as early as E6.5 (Fig. 6I,J). In some of the embryos, the extended area of *brachyury* expression revealed a broadening of the primitive streak, node and axial mesoderm domains. Frequently, mesoderm-like projections were observed growing out these areas (data not shown).

LPP3 inhibits β-catenin-mediated TCF transcriptional activity

Axis duplication in vertebrate embryos is associated with

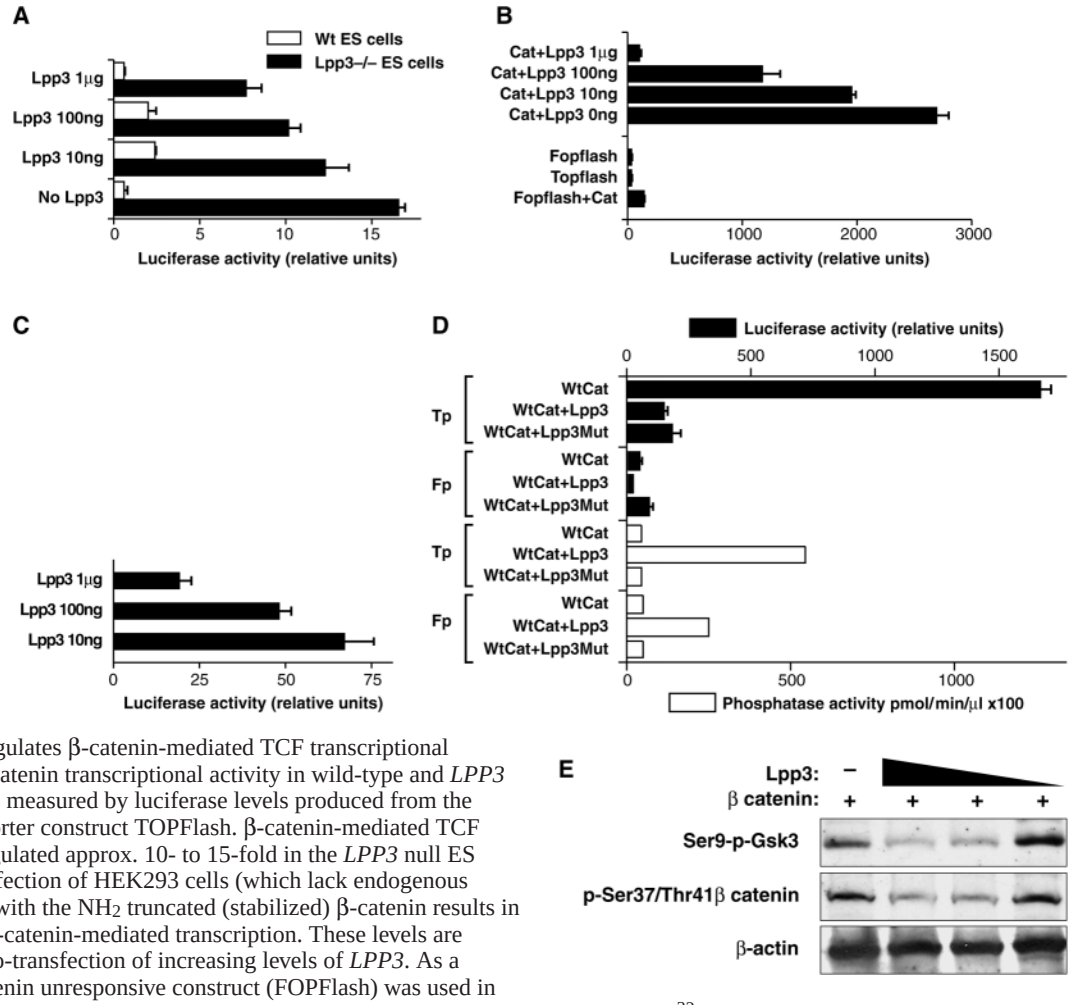

Fig. 7. LPP3 regulates β-catenin-mediated TCF transcriptional activity. (A) β-catenin transcriptional activity in wild-type and *LPP3* null ES cells, as measured by luciferase levels produced from the transfected reporter construct TOPFlash. β-catenin-mediated TCF activity is upregulated approx. 10- to 15-fold in the *LPP3* null ES cells. (B) Transfection of HEK293 cells (which lack endogenous *LPP3* activity) with the NH_2 truncated (stabilized) β-catenin results in high levels of β-catenin-mediated transcription. These levels are attenuated by co-transfection of increasing levels of *LPP3*. As a control, a β-catenin unresponsive construct (FOPFlash) was used in these experiments. *LPP3* activity in the transfected cells was verified by the release of ^{32}P from labeled LPA. (C) Increasing levels of transfected LPP3 also inhibits endogenous β-catenin-mediated transcription in the HEK293 cells. (D) Phosphatase-deficient LPP3 also inhibits β-catenin-mediated TCF transcription. HEK 293 cells transfected with TOPFlash reporter construct and an LPP3 expression cassette carrying the Ser197→Thr mutation that inactivates the phosphatase site inhibited TCF/β-catenin transcription. (E) Western analysis of extracts from the transfected cells in B show that higher concentrations of LPP3 decreased phosphorylation at Ser9 in GSK-3, which correlates with GSK-3 having an increased inhibitory effect on β-catenin. This coincides with the levels of β-catenin dephosphorylated at Ser37/Thr41 (the stabilized form) being reduced by increasing LPP3 levels.

alterations to the Wnt signaling pathways. Activation of the canonical Wnt signaling pathway, by Wnt ligand binding to the frizzled receptors, results in stabilization of β-catenin in the stimulated cells. Stabilization of β-catenin levels occurs by inhibiting the kinase activity of the axin-APC-GSK-3 complex that phosphorylates β-catenin with subsequent degradation of the phosphorylated β-catenin. Once β-catenin is stabilized it relieves transcriptional repression mediated by the TCF/Lef factors (Chan and Struhl, 2002; Staal et al., 2002).

The effect of LPP3 on Wnt signaling was analyzed by measuring β-catenin-mediated TCF transcription in the ES cells null for *LPP3*. In contrast to wild-type ES cells, the *LPP3* null cells exhibited a 10- to 15-fold increase in luciferase activity following transfection with the TCF-luciferase reporter plasmid (TOPFlash), a TCF/β-catenin responsive reporter gene (van de Wetering et al., 1997). The increased TOPflash activity was inhibited by about 50% following transfection of an *LPP3* expression cassette into the null ES cells (Fig. 7A).

In a converse series of experiments, an LPP3 expression construct was co-transfected into HEK293 cells which lack LPP3 activity, together with TOPFlash and either a wild-type or enhanced β-catenin expression vector, in which the latter construct lacked critical amino-terminal phosphorylation sites necessary for the degradation of β-catenin. As expected the β-catenin expression vectors, by themselves, strongly induced luciferase activity. However, co-transfection with LPP3 resulted in a reduction by up to 90% in reporter activity (Fig. 7B). HEK293 cells express endogenous β-catenin at low, but detectable levels, sufficient to induce detectable luciferase activity in transfected cells. These levels were also significantly reduced in the LPP3-transfected cells (Fig. 7C). *LPP3* activity in the transfected cells was verified by the release of ^{32}P from LPA labeled by diacylglycerol kinase (Fig. 7D). Increased LPP3 expression is therefore able to inhibit both exogenous and endogenous β-catenin transcriptional activity in HEK293 cells. Extracts from the transfected cells were probed by western analysis and revealed an inverse correlation between the levels of active wild-type β-catenin (dephosphorylated at

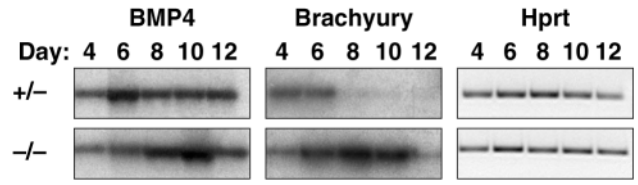

Fig. 8. Effect of *LPP3* in Wnt target gene expression. Expression analysis of Wnt target genes during EB differentiation. Semi-quantitative RT-PCR analysis of markers at the indicated days in culture. The loading control was the *Hprt* gene. *Bmp4* did not show significant differences in expression during EB differentiation. In contrast, while *brachyury* expression (a direct transcriptional target of the Wnt signaling pathway) decreased after 6 days in culture in heterozygous EBs, its expression was increased and prolonged in *LPP3*$^{-/-}$ EBs.

residues Ser37 and Thr41) and LPP3 levels (Fig. 7E). Furthermore, Ser9 phosphorylation of GSK-3 was reduced by increased LPP3 expression, possibly contributing to enhanced GSK-3-dependent inhibition of β-catenin (Fig. 7E).

To determine whether the inhibitory effect of LPP3 on β-catenin-mediated TCF transcription was dependent on the lipid phosphatase activity of the LPP3s, we used two different LPP3 constructs in which the phosphatase catalytic site had either been ablated by deleting 32 amino acids or mutated by changing serine 197→threonine (A.J.M., unpublished data). Both forms clearly lacked lipid phosphatase activity. The results presented in Fig. 7D show that LPP3, null for phosphatase activity, was as effective as the wild-type LPP3 at inhibiting β-catenin-mediated TCF transcription.

LPP3 deficiency affects anterior development and *Wnt* target gene expression

Increased activation of the Wnt/β-catenin signaling pathway induces axis duplication in the mouse (Popperl et al., 1997; Zeng et al., 1997). We therefore investigated whether *LPP3* loss of function maybe over-stimulating Wnt signaling in embryos. We analyzed the kinetics of expression of 3 *Wnt* regulated genes in differentiating heterozygous and homozygous *LPP3*-deficient EBs. Expression of bone morphogenetic protein (*Bmp4*; Fig. 8) and *nodal* (data not shown) was not affected, however *brachyury* expression was both elevated and prolonged in homozygous EBs compared with the heterozygotes (Fig. 8) consistent with the increased expression observed in some *LPP3*$^{-/-}$ embryos.

LPP3 is expressed in the anterior visceral endoderm (AVE) of early embryos, a tissue implicated in patterning of the early mouse embryo (Beddington and Robertson, 1999). AVE formation was affected in about 30% of the *LPP3* null embryos, which was revealed by abnormal expression of two markers of the AVE, specifically *Hex* and *dkk-1*. In normal embryos *dkk-1*, an extracellular antagonist of Wnt signaling, is expressed in a horseshoe-like pattern extending from the proximal to the lateral-distal AVE in wild-type and heterozygous E7.5 embryos (Glinka et al., 1998; Perea-Gomez et al., 2001; Zakin et al., 2000). Two out of 6 *LPP3* null embryos at equivalent stages showed reduction and abnormal expression of *dkk-1* transcripts (Fig. 6K). Although reduced levels of *dkk-1* expression were observed, the region of expression was more distal, with loss of expression occurring in the most proximal AVE. Furthermore an accumulation of *Hex*-positive cells in the distal tip was also observed in a subset of E7.0 null embryos. In the same null embryos *Wnt3* expression was detected in both the proximal anterior and posterior embryonic ectoderm. In normal E7.5 embryos *Wnt3* expression becomes restricted to the posterior embryo and primitive streak (Fig. 6L). Together, these results suggest that in the absence of LPP3, components regulating Wnt/β-catenin responses are both quantitatively and spatially altered, consistent with the abnormalities in axis patterning.

Murine *LPP3* has a ventralizing effect on *Xenopus* embryos

The loss of function of *LPP3* resulting in the duplication of axial structures (dorsalization) in the mouse embryo suggested that increased *LPP3* expression was having a ventralizing activity in vivo. To test this, murine *LPP3* mRNA was injected into the 2 dorsal blastomeres of 4-cell stage *Xenopus* embryos and subsequent larval development was analyzed. Synthesis and glycosylation of LPP3 protein was confirmed by western blot analysis of extracts from injected larvae (Fig. 9A,B). As controls, embryos were either injected with mLPP3 into their ventral blastomeres (Fig. 9C) or their dorsal blastomeres were injected with a mutated version of mLPP3 (lacking the same amino acids used to generate the phosphatase-deficient mutation). 80-100% of stage 22-24 embryos injected with 1-2.5 ng of *LPP3* mRNA in their dorsal or ventral blastomeres showed a phenotype consisting of the transient formation of a ‘blister’ in the ventral region of the developing larvae. In contrast, larvae injected with the mutated *mLPP3* were unaffected. These data suggested that *mLPP3* injection into frog embryos causes an ionic imbalance resulting in fluid accumulation under the skin that produces the blistered phenotype. However, as this phenotype appeared independent of the site of injection, it was not considered relevant for the analysis of LPP3 participation in axial patterning.

Stage 36 embryos, in which the dorsal blastomeres were injected with *LPP3* mRNA, formed an anterior-posterior (AP) axis, but with abnormal anterior development. They had a reduced forehead, small eyes that occasionally fused (cyclopia) and a reduced or missing cement gland (Fig. 9B, Table 3). In contrast, ventrally injected embryos developed normal anterior structures (Fig. 9C, Table 3). To analyze the extent of anterior abnormalities, several molecular markers were assayed in affected embryos by in situ hybridization or immunohistochemistry. *Xpax6* (an eye marker) and *Xotx2* (a forebrain and midbrain marker) probes revealed the absence and/or reduction of eyes and forebrain (Fig. 9D-F) whereas development of hindbrain (*Krox20*) and notochord (*Tor70*) were not affected (data not shown). The defects caused by

Table 3. Dorsal injection of murine LPP3 induces a ventralizing phenotype in *Xenopus* embryos

Mouse *LPP3* RNA (ng)	Injection site	Embryos injected	Embryos with microcephalic phenotype	%
0.4	Dorsal	40	20	50
1.0	Dorsal	59	50	85
1.0	Ventral	35	0	0
2.5	Dorsal	49	49	100
2.5	Ventral	29	5	17

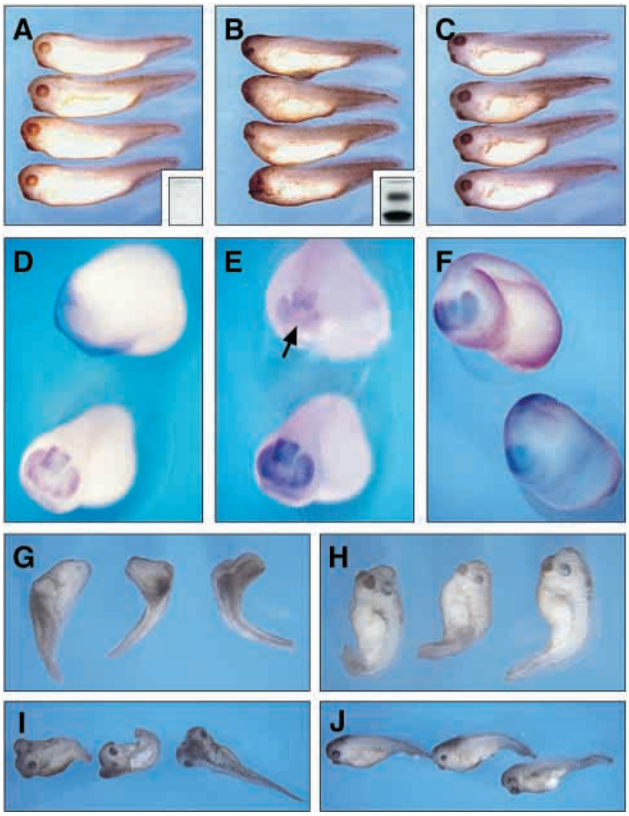

Fig. 9. Effect of *LPP3* in *Xenopus* axial patterning. (A-C) Effect of murine *LPP3* mRNA injection in *Xenopus* embryo development. Stage 36 larvae (A) uninjected, (B) injected dorsally or (C) ventrally with 1 ng of *mLPP3* mRNA. Inserts show translated LPP3 protein. Note that only the larvae injected dorsally had abnormal anterior development. (D-H) In situ hybridization of un-injected and dorsally injected *Xenopus* embryos with markers for anterior development (stage 22). (D,E) *Xotx2* detection in uninjected (bottom) and dorsally injected (top) embryos. Some injected embryos lacked (D) or had reduced (E) *Xotx2* expression. Reduced and fused eyes can be observed in the injected embryo (E, arrow). (F) *Xpax6* detection in uninjected (bottom) and dorsally injected (top) embryos. Injected embryos lacked distinguishable eye staining. (G) Embryos injected ventrally with *Xwnt3a* show a duplicated axis. (H) Co-injection of *mLPP3* with *Xwnt3a* mRNA rescues secondary axis formation but results in a weak dorsalizalized phenotype. (I) Axis duplication induced by ventral injection of *Xwnt8*. (J) Co-injection of *Xwnt8* with *LPP3* mRNA inhibited axis duplication, but the embryos still retained a weak dorsalization phenotype.

ectopic mLPP3 expression correspond to abnormalities 3-4 in the dorsoanterior index scale (Kao and Elinson, 1988), indicating a mild, but consistent, ventralizing activity of LPP3. The ventralizing activity of LPP3 was also analyzed by its ability to inhibit secondary axis formation induced by *Xwnt3a* and *Xwnt8*. Full-length *mLPP3* RNA co-injected with *Xwnt3a* or *Xwnt8* inhibited secondary axis formation, although the effect was not complete, with the majority of the embryos retaining a weak dorsalized phenotype (Fig. 9G-J and Table 4). Furthermore, LPP3 lacking phosphatase activity was also able to reduce the dorsalizing activity of Xwnt8, although not as effectively as full-length LPP3 (Table 4). These results strongly support a role for LPP3 in axis patterning through the regulation of Wnt signaling pathways.

Discussion

During early post-implantation murine development embryonic cell proliferation rapidly increases. Coincident with this increase is the onset of axis formation, gastrulation and appearance of the major tissue and organ primordia. Among the latter is the cardiovascular system that is essential to sustaining the supply of nutrients and oxygen to the embryo throughout subsequent development. In contrast to *LPP2* null embryos that develop normally (Zhang et al., 2000) we show that embryos lacking *LPP3*, exhibit profound defects in the development of the extra-embryonic vasculature and in embryonic axis formation. The effect of *LPP3* deficiency on vascularization and placental formation was fully penetrant on both a pure 129/S1 and mixed 129/S1×C57BL/6J backgrounds, whereas axis duplication was more prevalent on the mixed background implying the existence of genetic modifier(s) affecting the phenotypic outcome.

Development of the vascular system commences in the yolk sac and subsequently in the embryo proper by the formation of angioblasts in the cephalic and paraxial mesoderm. Angioblasts migrate and coalesce to form the primitive vascular plexus. Subsequent development of the system is by angiogenesis in which new vessels are formed by budding or sprouting from the vascular primordia. Thereafter maturation of the vascular system requires that vascular smooth muscle cells and pericytes are recruited to, and migrate around, the endothelial blood vessels to form the arteries, veins and capillaries (Carmeliet, 2000)

Many different peptide ligands and their receptors, including VEGF and its receptors, Flk1 and Flt1 (Ferrara et al., 1996; Fong et al., 1995; Shalaby et al., 1997; Shalaby et al., 1995), angiopoietin 1 and Tie 2 (Puri et al., 1995; Suri et al., 1996) PDGF-βB, the PDGF receptor β (Hellstrom et al., 1999), together with TGFβ1 (Dickson et al., 1995; Yang et al., 1999) are essential to the establishment, elaboration and maintenance of the cardiovascular system. Here we provide the first evidence that LPP3, an enzyme previously known to regulate bioactive phospholipids and/or their products is essential to some of the earliest stages in vascular development in the murine embryo. Embryos that were null for *LPP3* consistently

Table 4. LPP3 blocks axis duplication induced by Xwnt3a or Xwnt8 injection

Phenotype	Xwnt3a (%)	Xwnt3a/LPP3 (%)	Xwnt3a/mutant LPP3 (%)	Xwnt8 (%)	Xwnt8/LPP3 (%)	Xwnt8/mutant LPP3 (%)
Complete dorsalization	12/28 (43)	–	14/28 (50)	16/39 (41)	–	4/27 (15)
Axis duplication	16/28 (57)	16/50 (32)	14/28 (50)	23/39 (59)	4/43 (12)	16/27 (59)
Weak dorsalization	–	24/50 (48)	–	–	3/43 (79)	7/27 (26)
Normal	–	10/50 (20)	–	–	4/43 (9)	–

failed to establish an intact yolk sac and allantoic vasculature, with the allantois being unable to form an effective union with the chorion and the yolk sac endothelial cells failing to organize a vascular plexus. The allantois, which is derived by outgrowth of the extra-embryonic mesoderm from the proximal epiblast, did not extend towards and invade the chorion, but remained as a compact mass of tissue at the posterior of the embryo. An analysis of chimeras, in which the chorion was wild type and the entire embryo null for *LPP3* resulted in improved development of the mutant allantois with limited invasion of the chorion, although vascularization and the extent of invasion was still reduced compared to wild-type embryos. This revealed that chorionic expression of *LPP3* is required for proper growth and extension of the allantois. It is possible, by analogy with the role of *wunen* in regulating germ cell migration, that chorionic LPP3 may be regulating the production of some factor that guides the growth and extension of the allantois towards the chorion. However, endothelial cells of the yolk sac and allantois both express LPP3, and the inability of the null endothelial cells to organize and form vascular cords would appear to be cell autonomous and this may also affect outgrowth of the allantois. In chimeras made between wild-type embryos and *LPP3* null ES cells, where there was significant contribution of both genotypes to all embryonic tissues, it was noticeable that only a few *LPP3* null cells contributed to the umbilical vasculature, despite the allantois invading the chorion. The molecular basis for morphogenetic failure of the allantois remains obscure as neither the chorion nor allantois showed alterations in the levels or patterns of expression of the adhesive proteins VCAM1 and α4 integrin, both of which are essential to chorio-allantoic fusion (Gurtner et al., 1995; Yang et al., 1995). Failure of allantois outgrowth was also associated with an inability of the allantoic endothelial cells to organize and form the umbilical cord, suggesting that vasculogenesis in the allantois may be essential for its extension towards the chorion. This was strikingly demonstrated in the allantoic explants in which the wild-type endothelial cells organized into a network of cords, whereas those from null embryos, or wild-type embryos treated with the LPP inhibitor, propranolol, remained as a compact mass of PECAM1-positive cells.

These results are consistent with previous observations that lipid signaling pathways are essential to vasculogenesis and development of the cardiovascular system in later stage embryos. Treatment of cultured vascular endothelial cells with S1P induces adherens junction assembly and vascular morphogenesis (Lee et al., 1999) and these changes are mediated by binding of S1P to the $S1P_1$ and $S1P_3$ receptors. Likewise loss-of-function mutations in some of the S1P receptors are associated with failure in cardiovascular development in midgestation embryos. Also in the zebrafish, the mutation *miles apart* (*mil*), which affects a gene homologous to *S1P5* (a receptor for S1P), results in defective migration of cardiac precursor cells to the midline and failure of heart organogenesis (Kupperman et al., 2000). A loss-of-function mutation in the murine $S1P_1$ receptor results in hemorrhage and embryonic lethality at E12-14 as a consequence of incomplete vascular maturation, due to the failure of pericytes to respond to PDGF-induced cell migration and to surrounding the blood vessels (Hobson et al., 2001). Such mutations have implicated lipid signaling pathways in the maturation of the cardiovascular system, particularly with regard to phospholipids regulating cell migration and adhesive interactions, similar to the effects of phospholipids on germ-cell migration in the *Drosophila* mutant *wunen* (Starz-Gaiano et al., 2001; Zhang et al., 1997). In contrast our results with *LPP3* null mice suggest that lipid signaling pathways maybe required at an even earlier stage, specifically during morphogenesis of the umbilical and yolk sac vasculatures.

The role of *LPP3* in body axis patterning

Our results also revealed that *LPP3* influences axial patterning. Axis duplication in the mouse can be induced by node transplantation or by systemic administration of drugs affecting cytoskeletal organization during early gastrulation (Beddington, 1994; Kaufman and O'Shea, 1978). Similarly, activation of the Wnt signaling pathway induces axis duplication and embryonic dorsalization, e.g. by ectopic expression of *Cwnt8C* (Popperl et al., 1997). Interaction of the Wnt1 class of ligands (Wnt1, 3a, 8 and 8B) with the appropriate frizzled receptor inactivates the GSK-3-axin-APC complex with the subsequent stabilization of cytoplasmic β-catenin leading to the activation/repression of target genes. This is known as the canonical Wnt/β-catenin signaling pathway and when over stimulated, results in secondary axis formation in *Xenopus* embryos and transformation of mammary epithelial cells in the mouse (Miller et al., 1999).

The severe phenotype observed in 30% of $LPP3^{-/-}$ embryos is remarkably similar to mutations at the *fused* locus (Gluecksohn-Schoenheimer, 1949; Zeng et al., 1997). As with the $LPP3^{StwO3}$ mutation, *fused* mutations display variable expressivity and incomplete penetrance. Homozygotes for 4 alleles of the locus *Fu* (Caspari and David, 1940; Gluecksohn-Schoenheimer, 1949; Jacobs-Cohen et al., 1984; Perry et al., 1995) die around 8-10.5 days of gestation, showing a wide spectrum of abnormalities between embryos, including developmental delay, duplication of embryonic structures and development of parts of the embryo outside the amnion and yolk sac. The product of the *fused* locus, axin (Zeng et al., 1997), inhibits the signal transduction cascade activated by Wnts, by forming a complex with the β-catenin-phosphorylating form of GSK-3. In the absence of axin, GSK-3 is released from the β-catenin phosphorylating complex, resulting in the stabilization of β-catenin with activation of the canonical Wnt signaling response(s). The striking similarity between these phenotypes and the *LPP3* null phenotype strongly suggests that loss of *LPP3* may upregulate a canonical Wnt signaling response, with LPP3 functioning as a Wnt signaling antagonist in vivo.

Supporting this notion are four observations. First, *LPP3* expression inhibits TCF transcriptional activity mediated by both endogenous and exogenous β-catenin in HEK293 cells, probably by regulating the availability of the dephosphorylated and stable version of β-catenin. Secondly, consistent with the inhibitory action of *LPP3* on β-catenin, loss of *LPP3* resulted in a significant and marked increase in endogenous β-catenin activity in ES cells. Thirdly, loss of LPP3 results in an increased and sustained expression of the Wnt target gene *brachyury* in EBs (Yamaguchi et al., 1999), consistent with the expanded areas of expression in the primitive streak, node and axial mesoderm in the mutant embryos. The same alteration in

expression of *brachyury* occurs in mouse embryos either misexpressing *Cwnt8C* (Popperl et al., 1997) or following ectopic transplantation of the node, resulting in axis duplication with an extra row of somites between the two axes (Beddington, 1994). Lastly, the expression of the extracellular antagonist to Wnt signaling, *dkk1* (Glinka et al., 1998) overlaps with LPP3 in the anterior visceral endoderm (AVE). In some of the *LPP3* null embryos *dkk1* expression was reduced and altered in the AVE. Such alterations may also contribute to deregulated Wnt3 expression in the anterior embryonic ectoderm and anterior gene expression in the AVE leading to axis duplication (Perea-Gomez et al., 2002).

Additional evidence supporting the role of *LPP3* in axis patterning was derived from the expression of *LPP3* in *Xenopus* embryos. Ventralization or the reduction of axial structures is induced when some antagonists to the Wnt signaling pathway are injected into the dorsal blastomeres of *Xenopus* embryos (Cadigan and Nusse, 1997; Tago et al., 2000). Ectopic expression of murine *LPP3* in the dorsal blastomeres of *Xenopus* embryos caused a mild but clear ventralizing effect. In addition axis duplication, induced by injection of *Xwnt8* or *3a* mRNA, was mildly but consistently inhibited by co-injection of *LPP3* mRNA, directly demonstrating that *LPP3* affects axis patterning. Together the evidence strongly suggests that axis duplication in *LPP3*-deficient embryos arises as a result of increased activation of the canonical Wnt pathway, and an increase in β-catenin-mediated TCF transcription.

How LPP3 regulates β-catenin-mediated TCF transcription remains to be established. The surprising result from testing the LPP3 forms lacking phosphatase activity, was that they were equally effective as wild-type LPP3 at inhibiting TCF/β-catenin transcription in HEK293 cells. This revealed that LPP3 contains an additional, as yet undefined functional activity, which inhibits TCF/β-catenin activity.

Conclusions

Our results revealed that LPP3 is a multifunctional protein essential for different aspects of embryo development. In addition to its known lipid phosphatase activity, LPP3 may also regulate β-catenin activation by some, as yet undefined mechanism. However, given the multifunctional roles of LPP3 we propose that the phosphatase activity of LPP3 in regulating bioactive phospholipids levels may be critical to the vascular phenotype. The phosphatase activity may also indirectly regulate Wnt signaling pathways.

Endothelial cell migration and/or cell adhesion are affected by changes in phospholipid levels particularly LPA. LPA promotes or inhibits cell migration, adhesion and cytoskeletal reorganization depending on the cell type and concentration of the lipid (Panetti et al., 2001). Our results showed that, with loss of LPP3, extracellular levels of LPA were increased by the LPP3 null cells and also intracellular levels of DAG were reduced, resulting in reduced protein kinase C (PKC) activation. Activated PKC is required for the morphogenesis of the vasculature (Tang et al., 1997; Xia et al., 1996). Furthermore, propanolol, an inhibitor of LPP3 phosphatase activity, blocked capillary morphogenesis in the allantois explants.

However, we cannot exclude the possibility that the vasculogenesis phenotype is also influenced by LPP3 affecting Wnt signaling, as several Wnt signaling mutants are known to affect vascular, allantois and placental development (Galceran et al., 1999; Ishikawa et al., 2001; Parr et al., 2001). A third possibility emerged in that a putative RDG-mediated adhesion function has been recently described for human LPP3 which may affect endothelial cell adhesion (Humtsoe et al., 2003), although such an RDG sequence has not been found in the mouse *LPP3*.

Certain aspects of the gastrulation phenotype may also be influenced by LPP3 regulating the Wnt/Ca^{2+} pathway (Kuhl et al., 2000; Miller et al., 1999; Slusarski et al., 1997). Stimulation of the Wnt/Ca^{2+} pathway by the non-canonical class of Wnts, e.g. Wnt5a, results in activation of PKC and CamKII via a G-protein-dependent increase in intracellular DAG. In *Xenopus* embryos, activation of the non-canonical pathway promotes cell movement, a reduction in cell adhesion and antagonizes the Wnt canonical pathway (Torres et al., 1996). Moreover, overactivation of the Wnt/Ca^{2+} pathway promotes a ventralized phenotype in *Xenopus* embryos, characterized by a shortening of the AP axis and abnormal anterior structures (Kuhl et al., 2000), characteristics also found in *Xenopus* embryos ectopically expressing the active phosphatase form of LPP3. Loss of LPP3 may therefore attenuate the Wnt/Ca^{2+} pathway resulting in increased activation of the canonical Wnt/β-catenin pathway, affecting cell migration required for proper morphogenesis during axis patterning. In the *LPP3*$^{-/-}$ mouse embryos, lack of LPP3 appeared to affect cell migration required for establishment of the AVE, as indicated by the distal accumulation of *Hex*-expressing cells in the gastrulating embryos. Lastly, the failure of the phosphatase-deficient form of LPP3 to affect anterior *Xenopus* development suggests that LPP3 phosphatase activity may regulate signaling pathways necessary for anterior development. Consistent with this possibility were the reduction in DAG levels and PKC activation in the *LPP3*$^{-/-}$ cells and the similarities in vascular phenotypes between *frizzled 5* (*Fzd5*) null embryos (a putative receptor for activation of the non-canonical pathway) and the LPP3 null mice. Loss of *Fzd5* function results in poor development of the yolk sac vascular plexus and a reduction in embryonic blood vessels in the labyrinthine placenta (Ishikawa et al., 2001).

Future experiments will centre on defining the regions of LPP3 that regulate these activities. Once identified it will be possible to derive mouse embryos carrying mutations specific to these different functions, so determining the exact role LPP3 has in these different developmental processes.

We wish to thank Lori Sewell for excellent maintenance of our mouse facility, Pentao Liu and Luc Leyns for providing the *wnt3* and *Xwnt8* plasmids respectively. Also Mark Lewandoski and Terry Yamaguchi for many fruitful discussions and the generous provision of reagents.

References

Abbondanzo, S. J., Gadi, I. and Stewart, C. L. (1993). Derivation of embryonic stem cell lines. *Methods Enzymol.* **225**, 803-823.

Barila, D., Plateroti, M., Nobili, F., Muda, A. O., Xie, Y., Morimoto, T. and Perozzi, G. (1996). The Dri 42 gene, whose expression is up-regulated during epithelial differentiation, encodes a novel endoplasmic reticulum resident transmembrane protein. *J. Biol. Chem.* **271**, 29928-29936.

Beddington, R. S. (1994). Induction of a second neural axis by the mouse node. *Development* **120**, 613-620.

Beddington, R. S. and Robertson, E. J. (1999). Axis development and early asymmetry in mammals. *Cell* **96**, 195-209.
Bligh, E. G. and Dyer, W. J. (1959). A rapid method of total lipid extraction and purification. *Can. J. Biochem. Physiol.* **37**, 911-917.
Cadigan, K. M. and Nusse, R. (1997). Wnt signaling: a common theme in animal development. *Genes Dev.* **11**, 3286-3305.
Carmeliet, P. (2000). Mechanisms of angiogenesis and arteriogenesis. *Nat. Med.* **6**, 389-395.
Caspari, E. and David, P. (1940). The inheritance of a tail abnormality in the house mouse. *J. Hered.* **31**, 427-431.
Chan, S. K. and Struhl, G. (2002). Evidence that Armadillo transduces wingless by mediating nuclear export or cytosolic activation of Pangolin. *Cell* **111**, 265-280.
Chun, J., Goetzl, E. J., Hla, T., Igarashi, Y., Lynch, K. R., Moolenaar, W., Pyne, S. and Tigyi, G. (2002). International Union of Pharmacology. XXXIV. Lysophospholipid receptor nomenclature. *Pharmacol. Rev.* **54**, 265-269.
Contos, J. J., Fukushima, N., Weiner, J. A., Kaushal, D. and Chun, J. (2000). Requirement for the lpA1 lysophosphatidic acid receptor gene in normal suckling behavior. *Proc. Natl. Acad. Sci. USA* **97**, 13384-13389.
Contos, J. J., Ishii, I., Fukushima, N., Kingsbury, M. A., Ye, X., Kawamura, S., Brown, J. H. and Chun, J. (2002). Characterization of lpa(2) (Edg4) and lpa(1)/lpa(2) (Edg2/Edg4) lysophosphatidic acid receptor knockout mice: signaling deficits without obvious phenotypic abnormality attributable to lpa(2). *Mol. Cell Biol.* **22**, 6921-6929.
Dickson, M. C., Martin, J. S., Cousins, F. M., Kulkarni, A. B., Karlsson, S. and Akhurst, R. J. (1995). Defective haematopoiesis and vasculogenesis in transforming growth factor-beta 1 knock out mice. *Development* **121**, 1845-1854.
Ferrara, N., Carver-Moore, K., Chen, H., Dowd, M., Lu, L., O'Shea, K. S., Powell-Braxton, L., Hillan, K. J. and Moore, M. W. (1996). Heterozygous embryonic lethality induced by targeted inactivation of the VEGF gene. *Nature* **380**, 439-442.
Fong, G. H., Rossant, J., Gertsenstein, M. and Breitman, M. L. (1995). Role of the Flt-1 receptor tyrosine kinase in regulating the assembly of vascular endothelium. *Nature* **376**, 66-70.
Fukushima, N. and Chun, J. (2001). The LPA receptors. *Prostaglandins* **64**, 21-32.
Galceran, J., Farinas, I., Depew, M. J., Clevers, H. and Grosschedl, R. (1999). Wnt3a$^{-/-}$-like phenotype and limb deficiency in Lef1(–/–)Tcf1(–/–) mice. *Genes Dev.* **13**, 709-717.
Glinka, A., Wu, W., Delius, H., Monaghan, A. P., Blumenstock, C. and Niehrs, C. (1998). Dickkopf-1 is a member of a new family of secreted proteins and functions in head induction. *Nature* **391**, 357-362.
Gluecksohn-Schoenheimer, S. (1949). The effects of a lethal mutation responsible for duplications and twinning in mouse embryos. *J. Exp. Zool.* 47-76.
Goetzl, E. J. and An, S. (1998). Diversity of cellular receptors and functions for the lysophospholipid growth factors lysophosphatidic acid and sphingosine 1-phosphate. *FASEB J.* **12**, 1589-1598.
Gurtner, G. C., Davis, V., Li, H., McCoy, M. J., Sharpe, A. and Cybulsky, M. I. (1995). Targeted disruption of the murine VCAM1 gene: essential role of VCAM-1 in chorioallantoic fusion and placentation. *Genes Dev.* **9**, 1-14.
Harlan, R. (1991). *In situ* hybridization: an improved whole mount method for *Xenopus* embryos. *Methods Cell Biol.* **36**, 685-695.
Hellstrom, M., Kaln, M., Lindahl, P., Abramsson, A. and Betsholtz, C. (1999). Role of PDGF-B and PDGFR-beta in recruitment of vascular smooth muscle cells and pericytes during embryonic blood vessel formation in the mouse. *Development* **126**, 3047-3055.
Hla, T. (2001). Sphingosine 1-phosphate receptors. *Prostaglandins* **64**, 135-142.
Hobson, J. P., Rosenfeldt, H. M., Barak, L. S., Olivera, A., Poulton, S., Caron, M. G., Milstien, S. and Spiegel, S. (2001). Role of the sphingosine-1-phosphate receptor EDG-1 in PDGF-induced cell motility. *Science* **291**, 1800-1803.
Hogan, B., Beddington, R., Costantini, F. and Lacy, E. (1994). *Manipulating the Mouse Embryo: A Laboratory Manual*. Cold Spring Harbor, NY: Cold Spring Harbor Laboratory Press.
Humtsoe, J. O., Feng, S., Thakker, G. D., Yang, J., Hong, J. and Wary, K. K. (2003). Regulation of cell-cell interactions by phosphatidic acid phosphatase 2b/VCIP. *EMBO J.* **22**, 1539-1554.
Ishii, I., Ye, X., Friedman, B., Kawamura, S., Contos, J. J., Kingsbury, M. A., Yang, A. H., Zhang, G., Brown, J. H. and Chun, J. (2002). Marked perinatal lethality and cellular signaling deficits in mice null for the two sphingosine 1-phosphate (S1P) receptors, S1P(2)/LP(B2)/EDG-5 and S1P(3)/LP(B3)/EDG-3. *J. Biol. Chem.* **277**, 25152-25159.
Ishikawa, T., Tamai, Y., Zorn, A. M., Yoshida, H., Seldin, M. F., Nishikawa, S. and Taketo, M. M. (2001). Mouse Wnt receptor gene Fzd5 is essential for yolk sac and placental angiogenesis. *Development* **128**, 25-33.
Jacobs-Cohen, R., Spiegelman, M., Cookingham, J. and Bennett, D. (1984). Knobbly, a new dominant mutation in the mouse that affects embryonic ectoderm organization. *Genet. Res.* **43**, 43-50.
Kai, M., Wada, I., Imai, S., Sakane, F. and Kanoh, H. (1997). Cloning and characterization of two human isozymes of Mg2+-independent phosphatidic acid phosphatase. *J. Biol. Chem.* **272**, 24572-24578.
Kanoh, H., Kai, M. and Wada, I. (1997). Phosphatidic acid phosphatase from mammalian tissues: discovery of channel-like proteins with unexpected functions. *Biochim. Biophys. Acta* **1348**, 56-62.
Kao, K. R. and Elinson, R. P. (1988). The entire mesodermal mantle behaves as Spemann's organizer in dorsoanterior enhanced Xenopus laevis embryos. *Dev. Biol.* **127**, 64-77.
Kaufman, M. H. and O'Shea, K. S. (1978). Induction of monozygotic twinning in the mouse. *Nature* **276**, 707-708.
Kuhl, M., Sheldahl, L. C., Malbon, C. C. and Moon, R. T. (2000). Ca(2+)/calmodulin-dependent protein kinase II is stimulated by Wnt and Frizzled homologs and promotes ventral cell fates in Xenopus. *J. Biol. Chem.* **275**, 12701-12711.
Kupperman, E., An, S., Osborne, N., Waldron, S. and Stainier, D. Y. (2000). A sphingosine-1-phosphate receptor regulates cell migration during vertebrate heart development [see comments]. *Nature* **406**, 192-195.
Lee, M. J., Thangada, S., Claffey, K. P., Ancellin, N., Liu, C. H., Kluk, M., Volpi, M., Sha'afi, R. I. and Hla, T. (1999). Vascular endothelial cell adherens junction assembly and morphogenesis induced by sphingosine-1-phosphate. *Cell* **99**, 301-312.
Lennon, G. G., Auffray, C., Polymeropoulos, M. and Soares, M. B. (1996). The I.M.A.G.E. Consortium: an integrated molecular analysis of genomes and their expression. *Genomics* **33**, 151-152.
Ligoxygakis, P., Strigini, M. and Averof, M. (2001). Specification of left-right asymmetry in the embryonic gut of Drosophila. *Development* **128**, 1171-1174.
Liu, G., Kleine, L. and Hebert, R. L. (1999). Advances in the signal transduction of ceramide and related sphingolipids. *Crit. Rev. Clin. Lab. Sci.* **36**, 511-573.
Liu, Y., Wada, R., Yamashita, T., Mi, Y., Deng, C. X., Hobson, J. P., Rosenfeldt, H. M., Nava, V. E., Chae, S. S., Lee, M. J. et al. (2000). Edg-1, the G protein-coupled receptor for sphingosine-1-phosphate, is essential for vascular maturation. *J. Clin. Invest.* **106**, 951-961.
Miller, J. R., Hocking, A. M., Brown, J. D. and Moon, R. T. (1999). Mechanism and function of signal transduction by the Wnt/beta-catenin and Wnt/Ca2+ pathways. *Oncogene* **18**, 7860-7872.
Olivera, A., Romanowski, A., Rani, C. S. and Spiegel, S. (1997). Differential effects of sphingomyelinase and cell-permeable ceramide analogs on proliferation of Swiss 3T3 fibroblasts. *Biochim. Biophys. Acta* **1348**, 311-323.
Panetti, T. S., Magnusson, M. K., Peyruchaud, O., Zhang, Q., Cooke, M. E., Sakai, T. and Mosher, D. F. (2001). Modulation of cell interactions with extracellular matrix by lysophosphatidic acid and sphingosine 1-phosphate. *Prostaglandins* **64**, 93-106.
Pappu, A. S. and Hauser, G. (1983). Propranolol-induced inhibition of rat brain cytoplasmic phosphatidate phosphohydrolase. *Neurochem. Res.* **8**, 1565-1575.
Parr, B. A., Cornish, V. A., Cybulsky, M. I. and McMahon, A. P. (2001). Wnt7b regulates placental development in mice. *Dev. Biol.* **237**, 324-332.
Perea-Gomez, A., Lawson, K. A., Rhinn, M., Zakin, L., Brulet, P., Mazan, S. and Ang, S. L. (2001). Otx2 is required for visceral endoderm movement and for the restriction of posterior signals in the epiblast of the mouse embryo. *Development* **128**, 753-765.
Perea-Gomez, A., Vella, F. D., Shawlot, W., Oulad-Abdelghani, M., Chazaud, C., Meno, C., Pfister, V., Chen, L., Robertson, E., Hamada, H. et al. (2002). Nodal antagonists in the anterior visceral endoderm prevent the formation of multiple primitive streaks. *Dev. Cell* **3**, 745-756.
Perry, W., III, Vasicek, T., Lee, J., Rossi, J., Zeng, L., Zhang, T., Tilghman, S. and Costantini, F. (1995). Phenotypic and molecular analysis of a transgenic insertional allele of the mouse fused locus. *Genetics* **141**, 321-332.
Popperl, H., Schmidt, C., Wilson, V., Hume, C. R., Dodd, J., Krumlauf, R. and Beddington, R. S. (1997). Misexpression of Cwnt8C in the mouse

induces an ectopic embryonic axis and causes a truncation of the anterior neuroectoderm. *Development* **124**, 2997-3005.

Puri, M. C., Rossant, J., Alitalo, K., Bernstein, A. and Partanen, J. (1995). The receptor tyrosine kinase TIE is required for integrity and survival of vascular endothelial cells. *EMBO J.* **14**, 5884-5891.

Roberts, R., Sciorra, V. A. and Morris, A. J. (1998). Human type 2 phosphatidic acid phosphohydrolases. Substrate specificity of the type 2a, 2b, and 2c enzymes and cell surface activity of the 2a isoform. *J. Biol. Chem.* **273**, 22059-22067.

Robertson, E. (1987). Embryo-derived stem cell lines. In *Teratocarcinomas and Embryonic Stem Cells: A Practical Approach* (ed. E. Robertson), pp. 72-112. Oxford: IRL Press.

Schlaeger, T. M., Qin, Y., Fujiwara, Y., Magram, J. and Sato, T. N. (1995). Vascular endothelial cell lineage-specific promoter in transgenic mice. *Development* **121**, 1089-1098.

Sciorra, V. A. and Morris, A. J. (1999). Sequential actions of phospholipase D and phosphatidic acid phosphohydrolase 2b generate diglyceride in mammalian cells. *Mol. Biol. Cell* **10**, 3863-3876.

Sciorra, V. A. and Morris, A. J. (2002). Roles for lipid phosphate phosphatases in regulation of cellular signaling. *Biochim. Biophys. Acta* **1582**, 45-51.

Shalaby, F., Ho, J., Stanford, W. L., Fischer, K. D., Schuh, A. C., Schwartz, L., Bernstein, A. and Rossant, J. (1997). A requirement for Flk1 in primitive and definitive hematopoiesis and vasculogenesis. *Cell* **89**, 981-990.

Shalaby, F., Rossant, J., Yamaguchi, T. P., Gertsenstein, M., Wu, X. F., Breitman, M. L. and Schuh, A. C. (1995). Failure of blood-island formation and vasculogenesis in Flk-1-deficient mice. *Nature* **376**, 62-66.

Slusarski, D. C., Corces, V. G. and Moon, R. T. (1997). Interaction of Wnt and a Frizzled homologue triggers G-protein-linked phosphatidylinositol signalling. *Nature* **390**, 410-413.

Staal, F. J., Noort Mv, M., Strous, G. J. and Clevers, H. C. (2002). Wnt signals are transmitted through N-terminally dephosphorylated beta-catenin. *EMBO Rep.* **3**, 63-68.

Starz-Gaiano, M., Cho, N. K., Forbes, A. and Lehmann, R. (2001). Spatially restricted activity of a Drosophila lipid phosphatase guides migrating germ cells. *Development* **128**, 983-991.

Suri, C., Jones, P. F., Patan, S., Bartunkova, S., Maisonpierre, P. C., Davis, S., Sato, T. N. and Yancopoulos, G. D. (1996). Requisite role of angiopoietin-1, a ligand for the TIE2 receptor, during embryonic angiogenesis. *Cell* **87**, 1171-1180.

Tago, K., Nakamura, T., Nishita, M., Hyodo, J., Nagai, S., Murata, Y., Adachi, S., Ohwada, S., Morishita, Y., Shibuya, H. et al. (2000). Inhibition of Wnt signaling by ICAT, a novel beta-catenin-interacting protein. *Genes Dev.* **14**, 1741-1749.

Tang, S., Morgan, K. G., Parker, C. and Ware, J. A. (1997). Requirement for protein kinase C theta for cell cycle progression and formation of actin stress fibers and filopodia in vascular endothelial cells. *J. Biol. Chem.* **272**, 28704-28711.

Torres, M. A., Yang-Snyder, J. A., Purcell, S. M., DeMarais, A. A., McGrew, L. L. and Moon, R. T. (1996). Activities of the Wnt-1 class of secreted signaling factors are antagonized by the Wnt-5A class and by a dominant negative cadherin in early Xenopus development. *J. Cell Biol.* **133**, 1123-1137.

van de Wetering, M., Cavallo, R., Dooijes, D., van Beest, M., van Es, J., Loureiro, J., Ypma, A., Hursh, D., Jones, T., Bejsovec, A. et al. (1997). Armadillo coactivates transcription driven by the product of the Drosophila segment polarity gene dTCF. *Cell* **88**, 789-799.

Xia, P., Aiello, L. P., Ishii, H., Jiang, Z. Y., Park, D. J., Robinson, G. S., Takagi, H., Newsome, W. P., Jirousek, M. R. and King, G. L. (1996). Characterization of vascular endothelial growth factor's effect on the activation of protein kinase C, its isoforms, and endothelial cell growth. *J. Clin. Invest.* **98**, 2018-2026.

Yamaguchi, T. P., Takada, S., Yoshikawa, Y., Wu, N. and McMahon, A. P. (1999). T (Brachyury) is a direct target of Wnt3a during paraxial mesoderm specification. *Genes Dev.* **13**, 3185-3190.

Yang, J. T., Rayburn, H. and Hynes, R. O. (1995). Cell adhesion events mediated by alpha 4 integrins are essential in placental and cardiac development. *Development* **121**, 549-560.

Yang, X., Castilla, L. H., Xu, X., Li, C., Gotay, J., Weinstein, M., Liu, P. P. and Deng, C. X. (1999). Angiogenesis defects and mesenchymal apoptosis in mice lacking SMAD5. *Development* **126**, 1571-1580.

Yatomi, Y., Igarashi, Y., Yang, L., Hisano, N., Qi, R., Asazuma, N., Satoh, K., Ozaki, Y. and Kume, S. (1997). Sphingosine 1-phosphate, a bioactive sphingolipid abundantly stored in platelets, is a normal constituent of human plasma and serum. *J. Biochem (Tokyo)* **121**, 969-973.

Zakin, L., Reversade, B., Virlon, B., Rusniok, C., Glaser, P., Elalouf, J. M. and Brulet, P. (2000). Gene expression profiles in normal and Otx2–/– early gastrulating mouse embryos. *Proc. Natl. Acad. Sci. USA* **97**, 14388-14393.

Zambrowicz, B. P., Imamoto, A., Fiering, S., Herzenberg, L. A., Kerr, W. G. and Soriano, P. (1997). Disruption of overlapping transcripts in the ROSA beta geo 26 gene trap strain leads to widespread expression of beta-galactosidase in mouse embryos and hematopoietic cells. *Proc. Natl. Acad. Sci. USA* **94**, 3789-3794.

Zeng, L., Fagotto, F., Zhang, T., Hsu, W., Vasicek, T. J., Perry, W. L., 3rd, Lee, J. J., Tilghman, S. M., Gumbiner, B. M. and Costantini, F. (1997). The mouse Fused locus encodes Axin, an inhibitor of the Wnt signaling pathway that regulates embryonic axis formation. *Cell* **90**, 181-192.

Zhang, N., Sundberg, J. P. and Gridley, T. (2000). Mice mutant for Ppap2c, a homolog of the germ cell migration regulator wunen, are viable and fertile. *Genesis* **27**, 137-140.

Zhang, N., Zhang, J., Purcell, K. J., Cheng, Y. and Howard, K. (1997). The Drosophila protein Wunen repels migrating germ cells. *Nature* **385**, 64-67.

Zhang, W., Sakai, N., Fu, T., Okano, Y., Hirayama, H., Takenaka, K., Yamada, H. and Nozawa, Y. (1991). Diacylglycerol formation and DNA synthesis in endothelin-stimulated rat C6 glioma cells: the possible role of phosphatidylcholine breakdown. *Neurosci. Lett.* **123**, 164-166.